

Solvent Impact on the Diversity of Products in the Reaction of Lithium Diphenylphosphide and a Ti(III) Complex Supported by a *t*Bu₂P–P(SiMe₃) Ligand

A. Ziółkowska, N. Szykiewicz, J. Pikies, and Ł. Ponikiewski*

Cite This: *Inorg. Chem.* 2020, 59, 11305–11315

Read Online

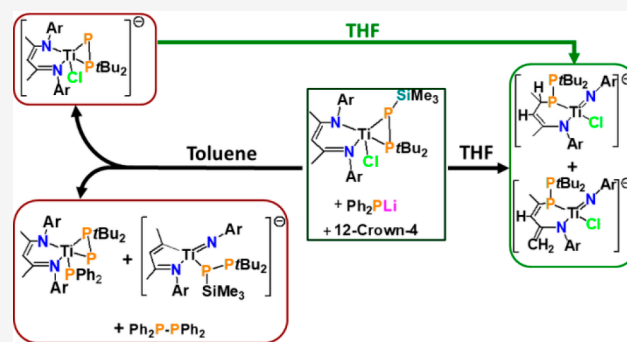
ACCESS |

Metrics & More

Article Recommendations

Supporting Information

ABSTRACT: We present two important trends in the reactivity of the titanium complex $[\text{Me}^c\text{NacNacTi}(\text{Cl})\{\eta^2\text{-P}(\text{SiMe}_3)\text{-P}t\text{Bu}_2\}]$ ($\text{Me}^c\text{NacNac}^- = [\text{Ar}]\text{NC}(\text{Me})\text{CHC}(\text{Me})\text{N}[\text{Ar}]$; $\text{Ar} = 2,6\text{-}i\text{Pr}_2\text{Ph}$) with nucleophilic reagents RLi ($\text{R} = \text{Ph}_2\text{P}$, $t\text{BuO}$, $(\text{Me}_3\text{Si})_2\text{N}$, and $t\text{Bu}_2\text{N}$) depending on the reaction medium. Reaction in nonpolar solvent (toluene) leads to three main products: via an autoredox process and nucleophilic substitution at the Ti-atom to afford the Ti(IV) complex $[\text{Me}^c\text{NacNacTi}(\text{R})\{\eta^2\text{-P}(\text{SiMe}_3)\text{-P}t\text{Bu}_2\}]$ (1 for $\text{R} = \text{PPh}_2$), via the elimination of Me_3SiR to afford Ti(III) complex $[\text{Me}^c\text{NacNacTi}(\text{Cl})\{\eta^2\text{-P}(\text{SiMe}_3)\text{-P}t\text{Bu}_2\}]^-[\text{Li}(12\text{-crown-}4)_2]^+$ (2), and via $2e^-$ reduction process to afford new ionic complex $[\{\text{ArNC}(\text{Me})\text{-CHC}(\text{Me})\}\text{Ti}=\text{NAr}\{\eta^1\text{-P}(\text{SiMe}_3)\text{-P}t\text{Bu}_2\}]^-[\text{Li}(12\text{-crown-}4)_2]^+$ (3). Quite differently, the complex $[\text{Me}^c\text{NacNacTi}(\text{Cl})\{\eta^2\text{-P}(\text{SiMe}_3)\text{-P}t\text{Bu}_2\}]$ reacts with Ph_2PLi in THF, unexpectedly yielding two new, four-coordinate Ti(IV) imido complexes **4a** $[\{\text{ArNC}(\text{Me})=\text{CHC}(\text{H})(\text{Me})\text{-P}(\text{P}t\text{Bu}_2)\}\text{Ti}=\text{NAr}(\text{Cl})]^-[\text{Li}(12\text{-crown-}4)_2]^+(\text{toluene})_2$ and **4b** $[\{\text{ArNC}(\text{CH}_2)\text{CH}=\text{C}(\text{Me})\text{-P}(\text{P}t\text{Bu}_2)\}\text{Ti}=\text{NAr}(\text{Cl})]^-[\text{Li}(12\text{-crown-}4)_2]^+(\text{Et}_2\text{O})$. Complex 2 dissolved in THF converts to **4a** and **4b**. **1**, **2**, **3**, **4a**, and **4b** were characterized by X-ray diffraction. **1**, **4a**, and **4b** were also fully characterized by multinuclear NMR spectroscopy.



1. INTRODUCTION

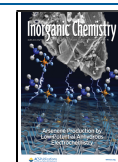
Recently, much attention has been dedicated to titanium carbene, nitrene and phosphinidene complexes.^{1–15} Due to the high oxo- and halogenophilicity of titanium in phosphinidene complexes, they exhibit significant phospho-Wittig reactivity.¹⁶ Thus, they are important synthons to introduce low-valent phosphorus fragments into organic molecules. The proper choice of auxiliary stabilizing ligands is very important for the synthesis of these complexes. Recently, β -diketiminato species have been widely applied as excellent stabilizing spectator ligands, especially for reactive organometallic compounds with low coordination numbers.^{17–20} Their additional advantages are the good crystallizing properties of the obtained complexes and the facile modification of these ligands.²¹ The stability of β -diketiminato ligands seems to be significantly overestimated and show a important contribution to reactivity. In the literature there are a wide range of processes in which the β -diketiminato ligands are directly involved and often present redox noninnocent behavior.^{22–24} Among others, two main transformations can be distinguished: electrophilic attack of the γ -carbon^{25,26} and deprotonation of the methyl group attached to the β -carbon of the NCCCN ring.^{27–32} Recently, the reductive transformation of a β -diketiminato ligand via migration of the imido group from the NacNac backbone to

the metal center and formation of a bond between the β -carbon and metal center was reported.^{28,33–36}

Our group has studied metathesis reactions of $\text{R}'\text{R}''\text{-P}(\text{SiMe}_3)\text{Li}$ with transition metal compounds bearing chloride ligands to introduce phosphanylphosphinidene $\text{R}'\text{R}''\text{-P-P}$ and phosphanylphosphido $\text{R}'\text{R}''\text{-P-P}(\text{SiMe}_3)$ moieties into the product complexes ($\text{R}' = t\text{Bu}$ and $i\text{Pr}$; $\text{R}'' = t\text{Bu}$, $i\text{Pr}$, and Ph). Phosphanylphosphido complexes have been obtained for titanium,^{37–39} iron,¹⁸ hafnium,⁴⁰ zirconium,^{40–42} tungsten,⁴³ and molybdenum,⁴⁴ and phosphanylphosphinidene complexes have been reported for titanium,^{37,39} zirconium,^{42,45} tungsten,^{46,47} molybdenum,⁴⁸ and platinum.^{49–52} Among these complexes, the complexes of titanium, zirconium, and iron were stabilized using a β -diketiminato ligand. The reactivity of the phosphanylphosphinidene complexes of tungsten was investigated by Grubba and co-workers.^{47,53} Moreover, the reactivities of monophosphorus analogues M-P and P-R are also rarely reported. In part, this may be caused by the

Received: March 18, 2020

Published: July 31, 2020



substituents R' on the phosphorus atom, which are generally alkyl or aryl groups, where the P–C bond is relatively robust. Hey-Hawkins and co-workers have made attempts to investigate reactivity of transition metal bis(trimethylsilyl)-phosphido complexes.⁵⁴

The reactivity of phosphanylphosphido complexes has practically not been studied. One of our recent work shows the reactivity of the titanium(III) complex containing *t*Bu₂P–P(SiMe₃) ligand toward selected chlorophosphanes (as electrophiles).⁵⁵ These research resulted in new method of synthesis of titanium(IV) complexes with versatile phosphanylphosphinidenes accompanied by the reduction of by-products which possess a new P–P bond, mainly symmetrical and unsymmetrical diphosphanes, or a P–H bond, *t*Bu₂PH in the great majority.⁵⁵

We considered it appropriate and justified to examine the reactivity toward reagents with other properties. In this report, we describe the reactions of β -diketiminate titanium(III) complex with phosphanylphosphido ligand (*t*Bu₂P–P(SiMe₃)) toward lithium nucleophiles such as Ph₂PLi, *t*Bu₂NLi, (Me₃Si)₂NLi, and *t*BuOLi in nonpolar (toluene) and polar (THF) solvents.

2. EXPERIMENTAL SECTION

Toluene, THF, and diethyl ether were dried over Na/benzophenone, and pentane was dried over Na/benzophenone/diglyme and distilled under argon. All reactions were performed under an argon atmosphere and were carried out under standard Schlenk techniques. Solution-phase ¹H, ³¹P, and ¹³C NMR spectra were recorded on a Bruker AV400 MHz (the external standards were tetramethylsilane for ¹H and ¹³C and 85% H₃PO₄ for ³¹P). Data were processed using Bruker's Topspin 3.5 software. Literature methods were used to prepare the titanium complex [Me₃NacNacTi(Cl){ η^2 -P(SiMe₃)-PtBu₂}].³⁷ (Me₃Si)₂NLi, *t*BuOLi, Ph₂PH, and *t*Bu₂NH were purchased from commercial suppliers. Ph₂PH and *t*Bu₂NH were lithiated and isolated as Ph₂PLi⁵⁶ and *t*Bu₂NLi⁵⁷ in our laboratory.

2.1. Reactions of [Me₃NacNacTi(Cl){ η^2 -P(SiMe₃)-PtBu₂}] with RLi Nucleophiles (R = Ph₂P, *t*BuO, (Me₃Si)₂N, and *t*Bu₂N) in the Presence of 12-crown-4 in Toluene. To a solution of [Me₃NacNacTi(Cl){ η^2 -P(SiMe₃)-PtBu₂}] (0.432 g; 0.550 mmol) in 20 mL of toluene cooled to –15 °C was added a suspension of Ph₂PLi (0.106 g; 0.550 mmol) in 10 mL of toluene. The bath temperature was increased to 0 °C, and at this temperature, the reaction solution was stirred for an additional 8 h. During this time, the color of the reaction mixture changed from green to red. Additionally, 12-crown-4 (0.194 g, 0.178 mL; 1,100 mmol; 1.089 g/mL) was added dropwise, and the reaction was stirred for 10 min at room temperature. Then, the solvent was removed under vacuum, and the dark red-green residue was washed with 10 mL of pentane, dried under reduced pressure, and dissolved in 20 mL of diethyl ether. The solution was filtered, concentrated to 10 mL, and stored at +4 °C. After 12 h, red crystals of [Me₃NacNacTi(Cl){ η^2 -P(SiMe₃)-PtBu₂}][Li(12-crown-4)]⁺ (**2**) appeared. Finally, we obtained 0.18 g (0.17 mmol, 31%). Anal. Calcd for C₅₃H₉₁ClLiN₂O₈P₂Ti: C, 61.41; H, 8.85; N, 2.70%. Found: C, 61.17; H, 8.68; N, 2.78%. Next, **2** was isolated, and the remaining solution was concentrated to 1 mL and stored at –25 °C. After 24 h, dark red crystals appeared, and they were characterized as [Me₃NacNacTi(PPh₂){ η^2 -P(SiMe₃)-PtBu₂}] (**1**). Finally, we obtained 0.13 g (0.16 mmol, 29%). Anal. Calcd for C₄₉H₆₉N₂P₂Ti: C, 71.17; H, 8.41; N, 3.39%. Found: C, 70.83; H, 8.34; N, 3.45%. ¹H NMR (C₆D₆) δ 8.29 (bt, 2H, PPh₂), 7.31 (bt, 2H, PPh₂), 7.21 (bm, 1H, PPh₂), 7.05 (bm, 3H, C₆H₃), 7.03 (s, 1H, C₆H₃), 6.98 (bt, 2H, PPh₂), 6.91 (d, 1H, J_{HH} = 2.4 Hz, C₆H₃), 6.89 (d, 1H, J_{HH} = 2.4 Hz, C₆H₃), 6.81 (bm, 1H, PPh₂), 6.59 (bt, 2H, PPh₂), 5.89 (s, 1H, γ -CH), 5.05 (sept, 2H, J_{HH} = 6.7 Hz, CHMe₂), 2.89 (sept, 2H, J_{HH} = 6.7 Hz, CHMe₂), 1.87 (s, 6H, C(Me)CHC(Me)), 1.72 (d, 6H, J_{HH} = 6.7 Hz, CHMe₂), 1.43 (d, 6H, J_{HH} = 6.7 Hz, CHMe₂), 1.31 (d, 6H, J_{HH} = 6.7 Hz, CHMe₂),

0.88 (d, 18H, J_{PH} = 14.8 Hz, P–PtBu₂), 0.79 (d, 6H, J_{HH} = 6.7 Hz, CHMe₂). ¹³C NMR (C₆D₆) δ 166.4 (C(Me)CHC(Me)), 143.8, 143.2, 142.8, 136.9, 129.9, 128.1, 126.9, 124.2, 123.9 (Ar–C), 100.2 (C(Me)CHC(Me)), 39.4 (PCMe₃), 32.3 (d, J_{CP} = 5.87, Me₃CP), 30.0 (s, PCHMe₂), 27.2 (s, PCHMe₂), 25.9 (s, C(Me)CHC(Me)), 25.5 (s, CHMe₂), 25.1 (s, CHMe₂), 24.7 (s, CHMe₂) ppm. ³¹P{¹H} NMR (C₆D₆) δ 676.7 ppm (dd, P–PtBu₂, J_{PP} = 472.3 Hz, J_{PP} = 14.5 Hz), 207.7 (dd, PPh₂, J_{PP} = 65.4 Hz, J_{PP} = 14.5 Hz), 104.0 (dd, P–PtBu₂, J_{PP} = 472.3 Hz, J_{PP} = 65.4 Hz) ppm.

The crystals of **1** were isolated, and the solvent was removed under vacuum. The dark orange-red oily residue was dissolved in 0.5 mL of diethyl ether. Additionally, a few drops of pentane were added. At the beginning, Schlenk was stored at –25 °C for 3 days and then at –40 °C. After 1 month, the oil had crystallized, and we obtained red crystals, which were measured and characterized as [ArNC(Me)CHC(Me)}Ti=NAr{ η^1 -P(SiMe₃)-PtBu₂}][Li(12-crown-4)]⁺ (**3**). Finally, we obtained 0.1 g (0.08 mmol, 15%, only the crystalline form has been isolated and weighed).

The reactions of [Me₃NacNacTi(Cl){ η^2 -P(SiMe₃)-PtBu₂}] with other nucleophiles (*t*Bu₂OLi, *t*Bu₂NLi, and (Me₃Si)₂NLi) were carried out analogously to this reaction with Ph₂PLi. In the reactions with these nucleophiles, the substitution products were not isolated in crystalline form; therefore, the reaction solutions were investigated by ³¹P{¹H} NMR spectroscopy. Complex **2** was only isolated product in the crystalline form in all reactions.

2.1.1. Reaction with *t*BuOLi. [Me₃NacNacTi(Cl){ η^2 -P(SiMe₃)-PtBu₂}] (0.240 g; 0.305 mmol), *t*BuOLi (0.024 g, 0.305 mmol), and 12-crown-4 (0.049 mL; 0.305 mmol). ³¹P{¹H} NMR (toluene-d₈) δ 669.6 (d, J_{PP} = 446.4 Hz, [Me₃NacNacTi(OtBu){ η^2 -P(SiMe₃)-PtBu₂}]), 86.8 (d, J_{PP} = 446.4 Hz, [Me₃NacNacTi(OtBu){ η^2 -P(SiMe₃)-PtBu₂}]), 44.2 (d, J_{PP} = 399.7 Hz, *t*Bu₂P–P(SiMe₃)₂), 19.6 (s, *t*Bu₂PH), 18.8 (d, J_{PP} = 190.7 Hz, *t*Bu₂P–P(SiMe₃)H), –198.2 (d, J_{PP} = 190.7 Hz, *t*Bu₂P–P(SiMe₃)H), –201.1 (d, J_{PP} = 399.7 Hz, *t*Bu₂P–P(SiMe₃)₂) ppm. Mass of isolated crystals of compound **2**: 0.065 g (0.06 mmol, 20%).

2.1.2. Reaction with *t*Bu₂NLi. [Me₃NacNacTi(Cl){ η^2 -P(SiMe₃)-PtBu₂}] (0.240 g; 0.305 mmol), *t*Bu₂NLi (0.041 g, 0.305 mmol), and 12-crown-4 (0.049 mL; 0.305 mmol). ³¹P{¹H} NMR (toluene-d₈) δ 539.3 (d, J_{PP} = 485.1 Hz, [Me₃NacNacTi(NtBu₂){ η^2 -P(SiMe₃)-PtBu₂}]), 87.0 (d, J_{PP} = 485.1 Hz, [Me₃NacNacTi(NtBu₂){ η^2 -P(SiMe₃)-PtBu₂}]), 44.3 (d, J_{PP} = 399.6 Hz, *t*Bu₂P–P(SiMe₃)₂), 19.7 (s, *t*Bu₂PH), 19.0 (d, J_{PP} = 190.4 Hz, *t*Bu₂P–P(SiMe₃)H), –197.3 (d, J_{PP} = 190.4 Hz, *t*Bu₂P–P(SiMe₃)H), –200.9; d, J_{PP} = 399.6 Hz, *t*Bu₂P–P(SiMe₃)₂) ppm. Mass of isolated crystals of compound **2**: 0.092 g (0.9 mmol, 29%).

2.1.3. Reaction with (Me₃Si)₂NLi. [Me₃NacNacTi(Cl){ η^2 -P(SiMe₃)-PtBu₂}] (0.240 g; 0.305 mmol), (Me₃Si)₂NLi (0.051 g, 0.305 mmol), and 12-crown-4 (0.049 mL; 0.305 mmol). ³¹P{¹H} NMR (toluene-d₈) δ 669.4 (d, J_{PP} = 441.4 Hz, [Me₃NacNacTi(N(SiMe₃)₂){ η^2 -P(SiMe₃)-PtBu₂}]), 86.8 (d, J_{PP} = 441.4 Hz, [Me₃NacNacTi(N(SiMe₃)₂){ η^2 -P(SiMe₃)-PtBu₂}]), 44.2 (d, J_{PP} = 400.1 Hz, *t*Bu₂P–P(SiMe₃)₂), 19.6 (s, *t*Bu₂PH), –201.1 (d, J_{PP} = 400.1 Hz, *t*Bu₂P–P(SiMe₃)₂) ppm. Mass of isolated crystals of compound **2**: 0.054 g (0.05 mmol, 17%).

2.2. Reactions of [Me₃NacNacTi(Cl){ η^2 -P(SiMe₃)-PtBu₂}] with Ph₂PLi in the Presence of 12-crown-4 in THF. Crystals of [Me₃NacNacTi(Cl){ η^2 -P(SiMe₃)-PtBu₂}] (0.320 g; 0.407 mmol) were dissolved in 10 mL of THF, and Ph₂PLi (0.078 g; 0.407 mmol) in 10 mL of THF was added at –15 °C. After approximately 5 min at room temperature, to the green-red solution was slowly added 12-crown-4 (0.112 mL; 0.814 mmol, 1.089 g/mL). The mixture changed color to deep-red. The mixture was stirred for 16 h, after which the solvent was evaporated. The obtained red solid was dissolved in the diethyl ether, but after 48 h at +4 °C, no crystals had appeared. The solvent was evaporated again, and crystallization was attempted in different solution mixtures. Depending on the solutions used to dissolve the obtained solid, different complexes were isolated.

2.2.1. Crystallization from Toluene/Pentane. The solid residue was dissolved in 10 mL of toluene, filtered, and concentrated to a volume of 3 mL. Then, 0.5 mL of pentane was added, and the solution was stored at +4 °C. After 24 h, red-brown crystals of complexes **4a** ([{(Ar)NC(Me)=CHC(H)(Me)(P–PtBu₂)}Ti=NAr(Cl)]⁺[Li(12-crown-4)]⁺(toluene)₂) and **4b** ([{(Ar)NC(CH₂)-

$\text{CH}=\text{C}(\text{Me})(\text{P}-\text{PtBu}_2)\text{Ti}=\text{NAr}(\text{Cl})^-[\text{Li}(12\text{-crown-}4)_2]^+(\text{Et}_2\text{O})$ were formed (yield for crystals 50%, 0.117 g).

NMR shifts for **4a**: ^1H NMR ($\text{THF}-d_8$) δ 7.07 (d, 1H, $m\text{-C}_6\text{H}_3$, $J_{\text{HH}} = 7.6$ Hz), 7.02 (d, 1H, $m\text{-C}_6\text{H}_3$, $J_{\text{HH}} = 7.5$ Hz), 6.81 (d, 1H, $m\text{-C}_6\text{H}_3$, $J_{\text{HH}} = 7.5$ Hz), 6.52 (d, 1H, $m\text{-C}_6\text{H}_3$, $J_{\text{HH}} = 7.5$ Hz), 6.35 (t, 1H, $p\text{-C}_6\text{H}_3$, $J_{\text{HH}} = 7.5$ Hz), 6.23 (t, 1H, $p\text{-C}_6\text{H}_3$, $J_{\text{HH}} = 7.5$ Hz), 4.73 (broad m, 1H, $\text{C}(\text{Me})=\text{CHC}(\text{H})(\text{Me})$), 4.03 (sept, 1H, CHMe_2 , $J_{\text{HH}} = 6.8$ Hz), 3.88 (sept, 1H, CHMe_2 , $J_{\text{HH}} = 6.7$ Hz), 3.74 (br. m, 1H, $\text{C}(\text{Me})=\text{CHC}(\text{H})(\text{Me})$), 3.64 (sept, 1H, CHMe_2 , $J_{\text{HH}} = 6.8$ Hz), 3.49 (s, 12-crown-4, 32H, CH_2), 3.38 (sept, 1H, CHMe_2 , $J_{\text{HH}} = 6.8$ Hz), 1.50 (d, 3H, $\text{C}(\text{Me})=\text{CHC}(\text{H})(\text{Me})(\text{P}-\text{PtBu}_2)$, $J_{\text{PH}} = 4.0$ Hz), 1.15 (d, 18H, $\text{P}-\text{PtBu}_2$, $J_{\text{PH}} = 10.4$ Hz), 1.07 (s, 3H, $\text{C}(\text{Me})=\text{CHC}(\text{H})(\text{Me})$), 0.95 (d, 6H, CHMe_2 , $J_{\text{HH}} = 6.8$ Hz), 0.92 (d, 6H, CHMe_2 , $J_{\text{HH}} = 6.8$ Hz), 0.89 (d, 6H, CHMe_2 , $J_{\text{HH}} = 6.8$ Hz), 0.58 (d, 6H, CHMe_2 , $J_{\text{HH}} = 6.7$ Hz). ^{13}C NMR ($\text{THF}-d_8$) δ 166.3 (s, $\text{C}(\text{Me})=\text{CHC}(\text{H})(\text{Me})$), 145.2 (s, $i\text{-C}_6\text{H}_3$), 143.0 (s, $i\text{-C}_6\text{H}_3$), 134.9 (s, $o\text{-C}_6\text{H}_3$), 131.5 (s, $o\text{-C}_6\text{H}_3$), 128.5 (s, $o\text{-C}_6\text{H}_3$), 125.0 (s, $m\text{-C}_6\text{H}_3$), 123.7 (s, $o\text{-C}_6\text{H}_3$), 123.6 (s, $m\text{-C}_6\text{H}_3$), 121.8 (s, $m\text{-C}_6\text{H}_3$), 121.6 (s, $m\text{-C}_6\text{H}_3$), 120.6 (s, $p\text{-C}_6\text{H}_3$), 117.6 (s, $p\text{-C}_6\text{H}_3$), 116.4 (s, $\text{C}(\text{Me})=\text{CHC}(\text{H})(\text{Me})$), 69.8 (s, 12-crown-4, CH_2), 55.0 (s, $\text{C}(\text{Me})=\text{CHC}(\text{H})(\text{Me})$), 33.8 (d, $\text{P}-\text{P}(\text{CMe}_3)_2$, $J_{\text{CP}} = 30.5$ Hz, $J_{\text{CP}} = 2.1$ Hz), 30.4 (d, $\text{P}-\text{P}(\text{CMe}_3)_2$, $J_{\text{CP}} = 16.0$ Hz), 28.6 (s, CHMe_2), 27.6 (s, CHMe_2), 27.2 (s, CHMe_2), 27.0 (s, CHMe_2), 25.4 (s, CHMe_2), 25.1 (s, $\text{C}(\text{Me})=\text{CHC}(\text{H})(\text{Me})$), 23.5 (s, CHMe_2), 23.3 (s, CHMe_2), 23.2 (s, CHMe_2), 23.1 (s, CHMe_2), 22.2 (s, $\text{C}(\text{Me})=\text{CHC}(\text{H})(\text{Me})$), 20.5 (s, CHMe_2), 13.4 (s, CHMe_2), 13.1 (s, CHMe_2). $^{31}\text{P}\{^1\text{H}\}$ NMR ($\text{THF}-d_8$) δ 34.4 (d, $\text{P}-\text{PtBu}_2$, $J_{\text{PP}} = 382.1$ Hz), -16.4 (d, $\text{P}-\text{PtBu}_2$, $J_{\text{PP}} = 382.1$ Hz) ppm.

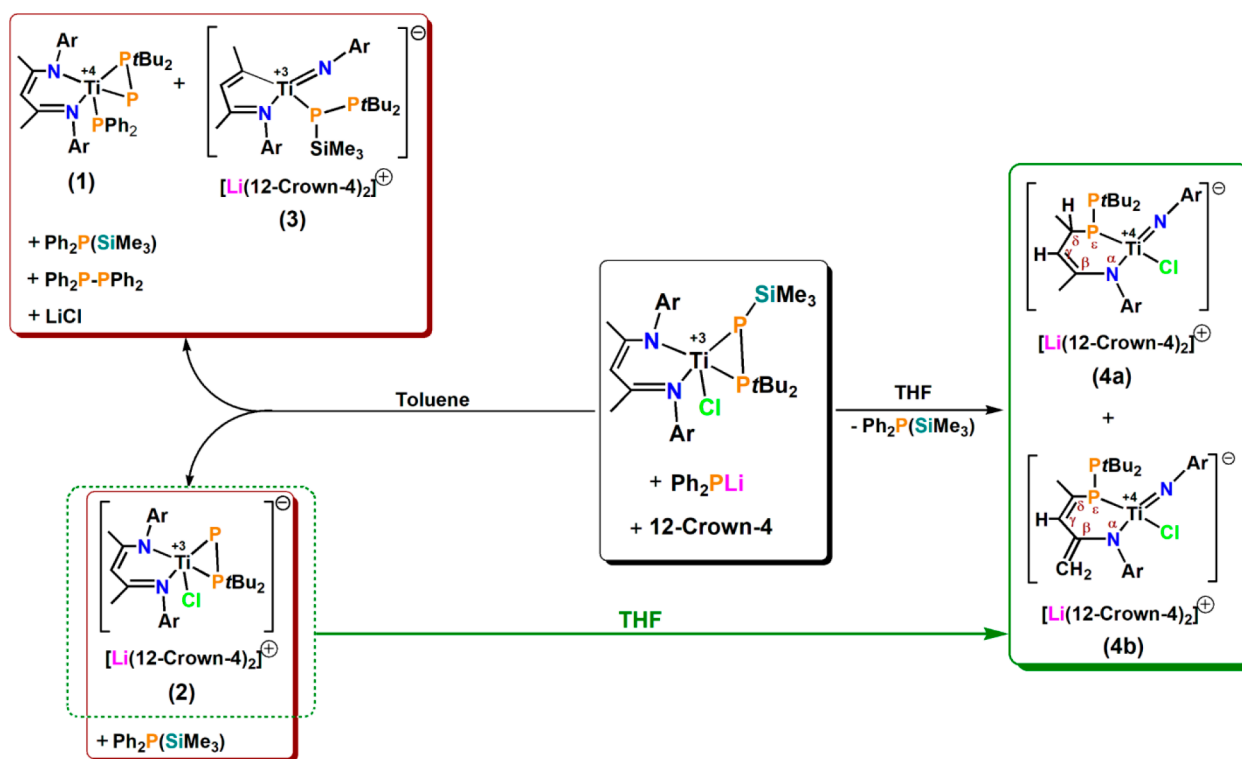
2.2.2. Crystallization from Diethyl Ether/Pentane. The solid residue was treated with 20 mL of diethyl ether, filtered, and concentrated to a volume of 5 mL. Next, 3 mL of pentane was added, and the solution was stored at $+4$ °C. After 5 h, dark red crystals of $[\{(\text{Ar})\text{NC}(\text{CH}_2)\text{CH}=\text{C}(\text{Me})(\text{P}-\text{PtBu}_2)\text{Ti}=\text{NAr}(\text{Cl})\}^-[\text{Li}(12\text{-crown-}4)_2]^+(\text{Et}_2\text{O})$ (**4b**) appeared. Yield of isolated crystals: 0.085 g (0.08 mmol, 38%) Anal. Calcd for $\text{C}_{57}\text{H}_{100}\text{ClLiN}_2\text{O}_9\text{P}_2\text{Ti}$: C, 61.70; H, 9.08; N, 2.52%. Found: C, 61.65; H, 8.91; N, 2.83%.

NMR shifts for **4b**: ^1H NMR ($\text{THF}-d_8$) δ 7.12 (d, 1H, $m\text{-C}_6\text{H}_3$, $J_{\text{HH}} = 7.7$ Hz), 6.77 (t, 1H, $p\text{-C}_6\text{H}_3$, $J_{\text{HH}} = 7.7$ Hz), 6.76 (d, 1H, $m\text{-C}_6\text{H}_3$, $J_{\text{HH}} = 7.8$ Hz), 6.73 (d, 1H, $m\text{-C}_6\text{H}_3$, $J_{\text{HH}} = 7.4$ Hz), 6.44 (d, 1H, $m\text{-C}_6\text{H}_3$, $J_{\text{HH}} = 7.6$ Hz), 6.21 (t, 1H, $p\text{-C}_6\text{H}_3$, $J_{\text{HH}} = 7.5$ Hz), 4.64 (s, 1H, $\text{C}(\text{CH}_2)\text{CH}=\text{C}(\text{Me})(\text{P}-\text{PtBu}_2)$), 4.34 (sept, 1H, CHMe_2 , $J_{\text{HH}} = 6.8$ Hz), 3.54 (sept, 1H, CHMe_2 , $J_{\text{HH}} = 6.7$ Hz), 3.54 (s, 12-crown-4, 32H, CH_2), 3.28 (q, 4H, $(\text{CH}_3\text{CH}_2)_2\text{O}$, $J_{\text{HH}} = 7.0$ Hz, $J_{\text{HH}} = 14.2$ Hz), 2.96 (broad signal, 1H, $\text{C}(\text{CH}_2)\text{CH}=\text{C}(\text{Me})(\text{P}-\text{PtBu}_2)$), 2.86 (sept, 1H, CHMe_2 , $J_{\text{HH}} = 6.6$ Hz), 2.63 (broad signal, 1H, $\text{C}(\text{CH}_2)\text{CH}=\text{C}(\text{Me})(\text{P}-\text{PtBu}_2)$), 2.32 (d, 3H, $\text{C}(\text{CH}_2)\text{CH}=\text{C}(\text{Me})(\text{P}-\text{PtBu}_2)$, $J_{\text{PH}} = 13.5$ Hz), 2.31 (sept, 1H, CHMe_2 , $J = 6.9$ Hz), 1.22 (d, 3H, CHMe_2 , $J_{\text{HH}} = 6.8$ Hz), 1.16 (d, 18H, $\text{P}-\text{PtBu}_2$, $J_{\text{PH}} = 10.7$ Hz), 1.11 (d, 3H, CHMe_2 , $J_{\text{HH}} = 6.8$ Hz), 1.03 (d, 3H, CHMe_2 , $J_{\text{HH}} = 6.9$ Hz), 1.01 (t, 6H, $(\text{CH}_3\text{CH}_2)_2\text{O}$, $J_{\text{HH}} = 7.1$ Hz), 0.98 (d, 3H, CHMe_2 , $J_{\text{HH}} = 6.8$ Hz), 0.91 (d, 3H, CHMe_2 , $J_{\text{HH}} = 6.8$ Hz), 0.90 (d, 3H, CHMe_2 , $J_{\text{HH}} = 6.8$ Hz), 0.85 (d, 3H, CHMe_2 , $J_{\text{HH}} = 6.8$ Hz), 0.55 (d, 3H, CHMe_2 , $J_{\text{HH}} = 6.7$ Hz). ^{13}C NMR ($\text{THF}-d_8$) δ 164.5 (d, $\text{C}(\text{CH}_2)\text{CH}=\text{C}(\text{Me})(\text{P}-\text{PtBu}_2)$, $J_{\text{CP}} = 44.2$ Hz), 156.5 (s, $i\text{-C}_6\text{H}_3$), 153.9 (s, $\text{C}(\text{CH}_2)\text{CH}=\text{C}(\text{Me})(\text{P}-\text{PtBu}_2)$), 150.7 (s, $i\text{-C}_6\text{H}_3$), 146.3 (s, $o\text{-C}_6\text{H}_3$), 143.5 (s, $o\text{-C}_6\text{H}_3$), 143.5 (s, $o\text{-C}_6\text{H}_3$), 142.2 (s, $o\text{-C}_6\text{H}_3$), 123.4 (s, $m\text{-C}_6\text{H}_3$), 123.2 (s, $m\text{-C}_6\text{H}_3$), 122.3 (s, $m\text{-C}_6\text{H}_3$), 122.0 (s, $p\text{-C}_6\text{H}_3$), 120.5 (s, $m\text{-C}_6\text{H}_3$), 117.8 (s, $p\text{-C}_6\text{H}_3$), 117.1 (s, $\text{C}(\text{CH}_2)\text{CH}=\text{C}(\text{Me})$), 77.0 (based on HMQC and ^{13}C -DEPT-135, d, $\text{C}(\text{CH}_2)\text{CH}=\text{C}(\text{Me})$, $J_{\text{CH}} = 132.1$ Hz), 69.8 (s, 12-crown-4, CH_2), 65.3 (s, $(\text{CH}_3\text{CH}_2)_2\text{O}$), 31.7 (dd, $\text{P}-\text{P}(\text{CMe}_3)_2$, $J_{\text{PC}} = 15.3$ Hz, $J_{\text{PC}} = 2.0$ Hz), 31.2 (d, $\text{C}(\text{CH}_2)\text{CH}=\text{C}(\text{Me})$, $J_{\text{PC}} = 13.8$ Hz), 31.0 (d, $\text{P}-\text{P}(\text{CMe}_3)_2$, $J_{\text{PC}} = 13.3$ Hz), 28.4 (s, CHMe_2), 27.8 (s, CHMe_2), 27.4 (s, CHMe_2), 26.6 (s, CHMe_2), 25.8 (s, CHMe_2), 24.5 (s, CHMe_2), 24.0 (s, CHMe_2), 23.8 (s, CHMe_2), 23.5 (s, CHMe_2), 23.4 (s, CHMe_2), 22.5 (s, CHMe_2), 21.9 (s, CHMe_2), 14.7 (s, $(\text{CH}_3\text{CH}_2)_2\text{O}$). $^{31}\text{P}\{^1\text{H}\}$ NMR ($\text{THF}-d_8$) δ 41.0 (d, $\text{P}-\text{PtBu}_2$, $J_{\text{PP}} = 307.1$ Hz), 28.5 (d, $\text{P}-\text{PtBu}_2$, $J_{\text{PP}} = 307.1$ Hz) ppm.

3. RESULTS AND DISCUSSION

3.1. Reactivity Study of $[\text{Me}_2\text{NacNacTi}(\text{Cl})\{\eta^2\text{-P}(\text{SiMe}_3)\text{-PtBu}_2\}]$ with Nucleophiles in the Nonpolar Solvent Toluene. Ti(III) complexes $[\text{Me}_2\text{NacNacTi}(\text{Cl})\{\eta^2\text{-P}(\text{SiMe}_3)\text{-PR}'\text{R}''\}]$ ($\text{R}' = t\text{Bu}$ and $i\text{Pr}$; $\text{R}'' = t\text{Bu}$, $i\text{Pr}$, and Ph) contain several atoms that are prone to nucleophilic substitution. The electrophilic Fukui functions f^+ calculated for three complexes, $[\text{Me}_2\text{NacNacTi}(\text{Cl})\{\eta^2\text{-P}(\text{SiMe}_3)\text{-PtBu}_2\}]$, $[\text{Me}_2\text{NacNacTi}(\text{Cl})\{\eta^2\text{-P}(\text{SiMe}_3)\text{-PiPr}_2\}]$, and $[\text{Me}_2\text{NacNacTi}(\text{Cl})\{\eta^2\text{-P}(\text{SiMe}_3)\text{-P}(\text{Ph})t\text{Bu}\}]$, indicate that the most electrophilic atoms in these molecules are the hard Ti-centers ($f^+ = 0.197$, 0.189 and 0.180, respectively).³⁹ Due to the theoretical results, we conducted the first reaction of $[\text{Me}_2\text{NacNacTi}(\text{Cl})\{\eta^2\text{-P}(\text{SiMe}_3)\text{-PtBu}_2\}]$ with Ph_2PLi at a 1:1 molar ratio in toluene. The reaction was started at -15 °C and then stirred for 8 h at 0 °C. The $^{31}\text{P}\{^1\text{H}\}$ NMR spectrum acquired 1 h after initiation of the reaction indicates that $\text{Ph}_2\text{P}(\text{SiMe}_3)$ (s, -56.7 ppm) is the dominant species in the reaction solution. The presence of this compound clearly indicates that nucleophilic substitution takes place at the softer silicon atom and that the SiMe_3 group is removed from the phosphido moiety. Surprisingly, the $^{31}\text{P}\{^1\text{H}\}$ NMR spectrum obtained 7 h later revealed that except for the signal of $\text{Ph}_2\text{P}(\text{SiMe}_3)$ a weaker set of resonances is visible. Additionally, a singlet at -14.9 ppm from the symmetrical diphosphane $\text{Ph}_2\text{P}-\text{PPh}_2$ is observed. The other signals observed in the spectrum can be confidently assigned to those of the new Ti(IV) complex $[\text{Me}_2\text{NacNacTi}(\text{P}^{(3)}\text{Ph}_2)\{\eta^2\text{-P}^{(1)}\text{-P}^{(2)}t\text{Bu}_2\}]$ (**1**) (d, 676.7 ppm, $J_{\text{P1P2}} = 472.3$ Hz, $J_{\text{P1P3}} = 14.5$ Hz, $\text{P}^{(1)}$; dd, 207.7 ppm, $J_{\text{P2P3}} = 65.4$ Hz, $J_{\text{P1P3}} = 14.5$ Hz, $\text{P}^{(3)}$; dd, 104.0 ppm, $J_{\text{P1P2}} = 472.3$ Hz, $J_{\text{P2P3}} = 65.4$ Hz; $\text{P}^{(2)}$) (for $^{31}\text{P}\{^1\text{H}\}$ NMR spectrum of reaction mixture, see Figure S2). The $^{31}\text{P}\{^1\text{H}\}$ NMR spectrum confirms the nucleophilic attack of Ph_2P^- on the titanium center and the elimination of the chloride ion as LiCl . Additionally, during this reaction, the titanium atom is oxidized ($1e^-$ oxidation). All attempts to isolate the compounds observed in the NMR spectra failed. To obtain the complexes in a crystalline form, the reaction of $[\text{Me}_2\text{NacNacTi}(\text{Cl})\{\eta^2\text{-P}(\text{SiMe}_3)\text{-PtBu}_2\}]$ with Ph_2PLi in toluene was conducted in the presence of 12-crown-4 (molar ratio 1:1:2). Importantly, 12-crown-4 was added only 10 min before the end of the reaction. This modification allowed us to isolate the ionic Ti(III) complex $[\text{Me}_2\text{NacNacTi}(\text{Cl})\{\eta^2\text{-P}(\text{SiMe}_3)\text{-PtBu}_2\}]^-[\text{Li}(12\text{-crown-}4)_2]^+$ (**2**) in a crystalline form. After the isolation of **2**, the reaction solution was investigated by NMR spectroscopy. $^{31}\text{P}\{^1\text{H}\}$ NMR revealed that the Ti(IV) complex $[\text{Me}_2\text{NacNacTi}(\text{PPh}_2)\{\eta^2\text{-P}-\text{PtBu}_2\}]$ (**1**) was still present in the reaction mixture; therefore, the solution was concentrated and stored at -25 °C. After 24 h, dark red crystals had appeared and were characterized as complex **1** by $^{31}\text{P}\{^1\text{H}\}$ NMR spectroscopy. $^1\text{H}/^{31}\text{P}$ -HMBC examinations of **1** revealed that the phosphanyl phosphorus atom (104.0 ppm) is only correlated with the *tert*-butyl groups (0.88 ppm, d, $J_{\text{PH}} = 14.8$ Hz, 18H), while the phosphido phosphorus atom (at 207.7 ppm) correlates with the protons at 8.29 ppm (broad signal), 6.59 ppm (broad signal), 5.89 ppm (s), 2.89 ppm (weak correlation, sept, $J_{\text{HH}} = 6.7$ Hz), and 1.87 ppm (s). The integrations of the above-mentioned proton signals indicate 6 H in the signal at 1.87 ppm, 1 H in the signal at 5.89 ppm and 2 H in the signal at 2.89 ppm (methyl group, γ -proton, and isopropyl group of the Me_2NacNac skeleton, respectively) (for the spectra of complex **1**, see Figures S3–S10). In the next step, the crystals of **1** were isolated, and the solvent was

Scheme 1. Summary of the Reagents and Products of the Reactions of $[\text{M}^e\text{NacNacTi}(\text{Cl})\{\eta^2\text{-P}(\text{SiMe}_3)\text{-PtBu}_2\}]$ with Ph_2PLi and 12-crown-4 in Different Solvents (Toluene and THF)



removed under vacuum. The obtained dark orange-red oily residue was dissolved in the mixture of diethyl ether and small amount of pentane. Storage at $-40\text{ }^\circ\text{C}$ for 1 month allowed us to obtain the oily residue in crystalline form. The X-ray measurement revealed that the complex $[\{\text{ArNC}(\text{Me})\text{CHC}(\text{Me})\}\text{Ti}=\text{NAr}\{\eta^1\text{-P}(\text{SiMe}_3)\text{-PtBu}_2\}][\text{Li}(12\text{-crown-4})_2]^+$ (3) was also created (for the molecular structure of complex 3, see Figure S1). NMR and X-ray results indicated that the reaction of $[\text{M}^e\text{NacNacTi}(\text{Cl})\{\eta^2\text{-P}(\text{SiMe}_3)\text{-PtBu}_2\}]$ with Ph_2PLi in the presence of 12-crown-4 in toluene probably leads to two independent and competitive reactions. The first reaction can be recognized as a lithiation of the phosphido phosphorus atom of the starting titanium(III) complex and proceeds without changing of the oxidation state of the titanium atom. The second reaction can be recognized as the redox reaction in which the new complexes 1, 3, and $\text{Ph}_2\text{P-PPh}_2$ are created. The molecular structure of complex 3 indicates that it is a product of $2e^-$ reduction of $[\text{M}^e\text{NacNacTi}(\text{Cl})\{\eta^2\text{-P}(\text{SiMe}_3)\text{-PtBu}_2\}]$. Mindiola and co-workers observed similar $2e^-$ reduction process of β -diketimate titanium(III) and zirconium(IV) complexes in the reactions with KC_8 .^{35,58} Tokitoh and co-workers received similar results with the same reagent for β -diketimate tetravalent complexes of metals of Ti-group.⁵⁹ In our previous research work, the reduction process of β -diketimate ligand was observed in the spontaneous transformation of $[\text{M}^e\text{NacNacTi}(\text{Cl})\{\eta^2\text{-P}(\text{SiMe}_3)\text{-PtBu}_2\}]$ into two complexes $[\text{M}^e\text{NacNacTi}(\text{Cl})\{\eta^2\text{-P-PtBu}_2\}]$ (oxidation product) and $[\{\text{ArNC}(\text{Me})\text{CHC}(\text{Me})\}\text{Ti}=\text{NAr}\{\eta^1\text{-P}(\text{SiMe}_3)\text{-PtBu}_2\}][\text{Li}(\text{THF})_2]^+$ (reduction product).³⁷ In this work, the formation of complex 3 may be coupled with two oxidation processes. One of these is the formation of titanium(IV)

complex 1, which can be viewed as $1e^-$ oxidation process of starting complex $[\text{M}^e\text{NacNacTi}(\text{Cl})\{\eta^2\text{-P}(\text{SiMe}_3)\text{-PtBu}_2\}]$ or $[\text{M}^e\text{NacNacTi}(\text{PPh}_2)\{\eta^2\text{-P}(\text{SiMe}_3)\text{-PtBu}_2\}]$ in the presence of Ph_2PLi . However, in the $^{31}\text{P}\{^1\text{H}\}$ NMR spectrum the signals of $[\text{M}^e\text{NacNacTi}(\text{Cl})\{\eta^2\text{-P-PtBu}_2\}]$ were never observed, which may indicate that in the first step the nucleophilic attack of Ph_2P^- on the titanium center occurs and results in this titanium(III) complex $[\text{M}^e\text{NacNacTi}(\text{PPh}_2)\{\eta^2\text{-P}(\text{SiMe}_3)\text{-PtBu}_2\}]$ being oxidized. The second process is connected with the $1e^-$ oxidation of Ph_2P^- that are still present in the reaction solution and creation of $\text{Ph}_2\text{P}^\cdot$ radicals and results in formation of a symmetrical $\text{Ph}_2\text{P-PPh}_2$. In these redox processes, $\text{Ph}_2\text{P}(\text{SiMe}_3)$ and LiCl are also formed. The above-described results are summarized in Scheme 1.

It should be emphasized that the employed reaction conditions aimed to optimize the preparation of compound 1. The reaction carried out in room temperature showed that the dominant processes were the elimination reaction of the SiMe_3 group and lithiation of phosphorus atom. In this case, compound 1 was formed in trace amounts, and its isolation in crystalline form was impossible. The key element in this case was also the time of addition of a crown ether. The addition of a 12-crown-4 at the beginning of the reaction favors the formation of complex 2; therefore, a crown ether was added almost at the end of the reaction.

Moreover, this reaction was also conducted with other nucleophilic reagents: $t\text{BuOLi}$, $(\text{Me}_3\text{Si})_2\text{NLi}$, and $t\text{Bu}_2\text{NLi}$. After each of these reactions, we only isolated paramagnetic complex 2. Furthermore, the formation of 2 was accompanied by the creation of products containing SiMe_3 groups (visible in the ^1H NMR spectrum as $t\text{BuO}(\text{SiMe}_3)$ at 1.25 ppm (s) and

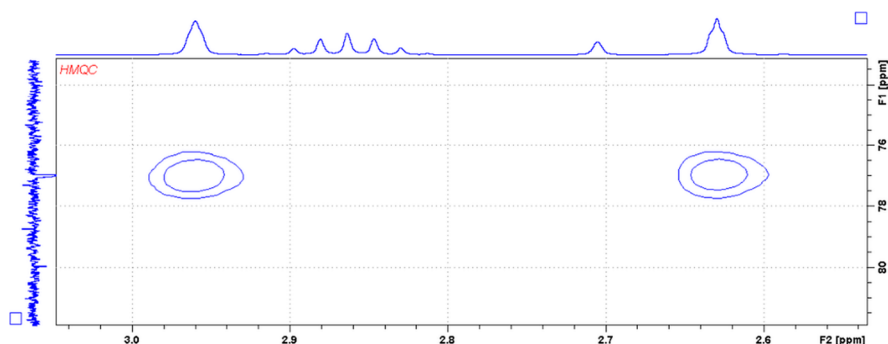


Figure 1. HMQC spectrum ($^1\text{H}/^{13}\text{C}$ -DEPT-135) showing the correlation of the sp^2 -hybridized carbon atom with protons.

0.05 ppm (s); $(\text{Me}_3\text{Si})_3\text{N}$ at 0.11 ppm (s); and $t\text{Bu}_2\text{N}(\text{SiMe}_3)$ at 1.32 ppm (s), 1.24 ppm (s) and 0.1 ppm (s), respectively). Additionally, $^{31}\text{P}\{^1\text{H}\}$ NMR examination of the reaction solution also revealed the formation of Ti(IV) complexes due to nucleophilic substitution of the Cl functionality on Ti atom by the RLi nucleophile ($\text{R} = \text{N}(\text{SiMe}_3)_2$, $t\text{BuO}$, and $t\text{Bu}_2\text{N}$): $[\text{Me}^e\text{NacNacTi}(\text{OtBu})\{\eta^2\text{-P}^{(1),(2)}t\text{Bu}_2\}]$ (d, (P1) 669.6 ppm and (P2) 86.8 ppm, $J_{\text{PP}} = 446.4$ Hz), $[\text{Me}^e\text{NacNacTi}(\text{N}t\text{Bu}_2)\{\eta^2\text{-P}^{(1),(2)}t\text{Bu}_2\}]$ (d, (P1) 539.3 ppm and (P2) 87.0 ppm, $J_{\text{PP}} = 485.1$ Hz), and $[\text{Me}^e\text{NacNacTi}\{\text{N}(\text{SiMe}_3)_2\}\{\eta^2\text{-P}^{(1),(2)}t\text{Bu}_2\}]$ (d, (P1) 669.4 ppm and (P2) 86.8 ppm, $J_{\text{PP}} = 441.4$ Hz) (for the $^{31}\text{P}\{^1\text{H}\}$ NMR spectra of reaction mixture, see Figures S14–S16). Unfortunately, the amounts of the titanium(IV) complexes were much smaller than what was generated in the reaction with Ph_2PLi . Additionally, modification of the reaction conditions did not increase the amounts of the nucleophilic substitution products. We also observed the formation of diphosphane $t\text{Bu}_2\text{P-P}(\text{SiMe}_3)_2$ in the reaction with $(\text{Me}_3\text{Si})_2\text{NLi}$ and $t\text{Bu}_2\text{NLi}$, which may indicate that in these reactions, the starting complex decomposes.

3.2. Reactivity Study of $[\text{Me}^e\text{NacNacTi}(\text{Cl})\{\eta^2\text{-P}(\text{SiMe}_3)\text{-PtBu}_2\}]$ with Nucleophiles in the Polar Solvent: THF. In view of the above obtained results for reactivity in a nonpolar solvent, we used only Ph_2PLi for reactivity in a polar solvent. The reaction of $[\text{Me}^e\text{NacNacTi}(\text{Cl})\{\eta^2\text{-P}(\text{SiMe}_3)\text{-PtBu}_2\}]$ with Ph_2PLi was also studied in THF in the presence of 12-crown-4 and a molar ratio of 1:1:2. Surprisingly, $[\text{Me}^e\text{NacNacTi}(\text{Cl})\{\eta^2\text{-P}(\text{SiMe}_3)\text{-PtBu}_2\}]$ reacts with Ph_2PLi quite differently under these conditions. The $^{31}\text{P}\{^1\text{H}\}$ NMR spectrum of the reaction mixture shows two AX patterns from two separate complexes: **4a** (34.4 ppm and -16.4 ppm, $J_{\text{PP}} = 382.1$ Hz) and **4b** (41.0 and 28.5 ppm, $J_{\text{PP}} = 307.1$ Hz). The observed signals indicate that in this reaction, the titanium oxidation state is changed from +3 to +4. Crystallization from toluene/pentane solution led exclusively to a mixture of **4a** and **4b** crystals (for all the NMR spectra of the mixture of **4a** and **4b**, see Figures S26–S36). The crystallization from diethyl ether/pentane after the reaction conducted in THF led immediately to complex **4b**. All attempts to isolate only complex **4a** were unsuccessful. **4b** was analyzed by X-ray crystallography and identified as $[\{(\text{Ar})\text{NC}(\text{CH}_2)\text{CH}=\text{C}(\text{Me})(\text{P-P}t\text{Bu}_2)\}\text{Ti}=\text{NAr}(\text{Cl})]^-[\text{Li}(12\text{-crown-4})_2]^+(\text{Et}_2\text{O})$. The X-ray-quality crystals of **4a** were picked from a mixture of crystals (**4a** and **4b**) and finally identified as $[\{(\text{Ar})\text{NC}(\text{Me})=\text{CHC}(\text{H})(\text{Me})(\text{P-P}t\text{Bu}_2)\}\text{Ti}=\text{NAr}(\text{Cl})]^-[\text{Li}(12\text{-crown-4})_2]^+(\text{toluene})_2$.

X-ray and NMR studies of **4a** and **4b** revealed the “phospha-Staudinger” displacement of the imide group N-Ar from

Me^eNacNac by the phosphanylphosphinidene $\text{P-P}t\text{Bu}_2$ moiety and an intermolecular hydrogen shift leading to two four-coordinate Ti(IV) imido complexes with different NP ligands. It should be noted that a similar displacement involving the imine-aryl functionality of the NacNac ligand has been described by Mindiola and co-workers.¹⁶ Additionally, in complexes **4a** and **4b**, the oxidation of both Ti atoms is accompanied by the reduction of the two putative hybrid NP ligands $[\text{P}(\text{P}t\text{Bu}_2)\text{-CH}(\text{Me})=\text{CH-C}(\text{Me})=\text{N}(\text{Ar})]$ derived from the Me^eNacNac anion (Scheme 1).

4a $[\{(\text{Ar})\text{NC}(\text{Me})=\text{CHC}(\text{H})(\text{Me})(\text{P-P}t\text{Bu}_2)\}\text{Ti}=\text{NAr}(\text{Cl})]^-[\text{Li}(12\text{-crown-4})_2]^+(\text{toluene})_2$ can be considered as a product of hydrogen addition to the δ -carbon atom in the NP hybrid ligand. The proton connected to the δ -carbon atom in **4a** is visible in the ^1H NMR spectrum as a broad multiplet at 3.74 ppm, and the signal of the δ -carbon atom appears in the ^{13}C NMR spectrum at 55.0 ppm (based on HMQC and ^{13}C -DEPT-90). An analogous reduction of a NacNac ligand via the addition of a hydrogen atom to the β -carbon of the backbone of the β -diketiminate ligand was observed by Uhl and co-workers. The reduction process was revealed in the reaction of NacNacH with AlH_3 and EtNMe_2 , in which the reduced ligand was formed by hydrogen atom transfer from aluminum to a β -carbon atom.⁶⁰ **4b** $[\{(\text{Ar})\text{NC}(\text{CH}_2)\text{CH}=\text{C}(\text{Me})(\text{P-P}t\text{Bu}_2)\}\text{Ti}=\text{NAr}(\text{Cl})]^-[\text{Li}(12\text{-crown-4})_2]^+(\text{Et}_2\text{O})$ can be considered as a product of hydrogen elimination from the Me group at the β -carbon atom in the NP hybrid ligand. In the ^1H NMR spectrum, the two protons of the methylene group are observed at 2.96 and 2.63 ppm. These resonances correlate to the sp^2 -hybridized carbon observed at 77.06 ppm (based on HMQC and ^{13}C -DEPT-135) (see Figure 1).

The signal of the γ -proton in **4b** is centered at 4.64 ppm. A similar deprotonation process of the β -diketiminate ligand in the titanium complex was reported by Mindiola and co-workers, although the reduction reaction was conducted with KCH_2Ph (4.92 ppm for the γ -proton and 3.64 and 3.25 ppm for CH_2).²⁸ It is worth noting that Mindiola and co-workers also reported approximate determination for a β -diketiminate ligand, which can interact with an adjacent phosphinidene ligand in a “phospha-Staudinger” reaction, generating a titanium-imide complex supported by the new NP ligand.⁶¹ Furthermore, both reduction reactions of the β -diketiminate ligands were previously described separately in the literature, but such a conjugated autoredox reaction has never been reported.

We also studied the progress of the reaction according to Scheme 1, i.e., the formation of **4a** and **4b** over time directly in an NMR tube. Therefore, the $[\text{Me}^e\text{NacNacTi}(\text{Cl})\{\eta^2\text{-P}(\text{SiMe}_3)\text{-}$

PtBu₂}] complex was stirred with Ph₂PLi and 12-crown-4 in THF at -15 °C. The ³¹P{¹H} NMR spectrum obtained immediately after mixing reveals only a strong singlet for Ph₂P(SiMe₃). ³¹P{¹H} NMR spectra were acquired after 1, 2, 24, 48, and 72 h, 7 days, and 2 months (see Figures S39–S41). At 1 hour after initiation of the reaction at ambient temperature, the ³¹P{¹H} NMR spectrum showed weak signals of **4a** and **4b**. Between 1 and 48 h, we observed the amplification of the signals of **4a** and **4b**, and maximum signals of **4a** and **4b** were observed 48 h after the initiation of the reaction. Further measurements revealed a decrease in the intensity of the signals for **4a** and complete disappearance after 2 months. Unlike **4a**, complex **4b** is stable in THF solution. Interestingly, we observed that the singlets at 196.1 ppm (²J_{P-H} = 14.5 Hz, determined from the ³¹P NMR spectrum) and 19.6 ppm (*t*Bu₂PH) increase with the reaction time, very likely due to the decomposition of **4a**. The ¹H/³¹P-HMBC spectrum indicates that the atom appearing at 196.1 ppm is conjugated to the protons observed at 6.42 ppm (d, J_{PH} = 5.9 Hz, 1H), 2.34 ppm (d, J_{PH} = 13.8 Hz, 3H), and 1.8 ppm (d, J_{PH} = 1.8 Hz, 3H). The integration of the above-mentioned protons reveals the following: Only 1 H is located at 6.42 ppm, 2.34 ppm represents 3 H, and 1.8 ppm represents 3 H. Additionally, in the ¹H/¹³C-HMBC spectrum, we observe the correlations of the protons located at 6.42 ppm with the carbon atom appearing at 118.2 ppm (J_{PC} = 6.3 Hz) and of the protons visible at 2.34 and 1.8 ppm with the carbons appearing at 13.5 ppm (d, J_{PC} = 10.6 Hz) and 14.4 ppm (d, J_{PC} = 4.3 Hz), respectively. The ¹H/¹³C-HMBC spectrum indicates that the protons at 2.34 and 1.8 ppm correlate with the carbon at 118.2 ppm. All NMR results show a signal near 196.1 ppm, which theoretically confirms the presence of a titanium(IV) complex with a PN ligand similar to that of **4a**. Unfortunately, all attempts to isolate this complex failed. In order to investigate the influence of temperature on the reaction route, we have carried out the above-described reaction again. The substrates were also mixed at -15 °C and immediately after mixing, the ³¹P{¹H} NMR spectrum was measured and singlet from Ph₂P(SiMe₃) was observed. The NMR tube was heated in the oily bath at +50 °C. Next, spectra were acquired after 1, 2, 24, 48, and 72 h and 7 days. The conducted experiment revealed that the temperature has an impact on the reaction rate. Higher temperature causes the reaction proceeded rapidly but no other products are formed. Moreover, after 7 days, complex **4a** is no longer visible in the solution.

To better identify the differences between the reactions in polar and nonpolar solvents, we also carried out reactions with the same amounts of substrates and under the same conditions (RT). In both reactions, 12-crown-4 was added at the beginning of the reactions. One reaction was carried out in toluene-*d*₈, while the other was carried out in THF-*d*₈. Reaction mixtures were sealed in NMR tubes and measured cyclically. Measurements were performed after 1, 24, and 48 h and 5 days from the initiation of the reactions. The conducted experiments revealed that in nonpolar solvent only complex **1** was visible in the ³¹P{¹H} NMR spectrum, while the high signal of Ph₂P(SiMe₃) indicated on the presence of complex **2** in the reaction mixture. Importantly, the ³¹P{¹H} NMR measurement conducted after 5 days revealed no signals from **4a** and **4b** (see Figure S42). The obtained results clearly show, that both complexes **1** and **2** are stable in the nonpolar solvent. In the reaction carried out in THF-*d*₈ formation of complexes **4a** and **4b** was observed, while the formation of complex **1** was

not observed (see Figure S43). These experiments clearly prove that the polarity of the solvents is very important in the reaction of [Me₂NacNacTi(Cl)](η²-P(SiMe₃)-PtBu₂) with Ph₂PLi and 12-crown-4 and has a direct impact on the resulting products.

Finally, we also examined the stability of isolated crystals of **2** in THF at room temperature over 24 h. Therefore, the crystals of **2** were dissolved in THF-*d*₈ and investigated via NMR. The ³¹P{¹H} NMR spectrum revealed the formation of complexes **4a** and **4b** (Scheme 1). Additionally, in the ¹H NMR spectrum the proton connected to the β-carbon was also visible (see Figures S44 and S45). Obtained results may indicate that the protonation of the β-carbon in **4a** is directly connected with deprotonation process observed in complex **4b**. In this intermolecular process of two molecules of complex **2**, in the “phosha-Staudinger, protonation and deprotonation reactions, the one molecule of complex **4a** and one molecule of complex **4b** are created.

3.3. X-ray Structural Analysis. Complex **1** crystallized in the orthorhombic space group *Pnma* with four molecules in the unit cell. **1** displays a five-coordinate titanium complex with pseudosquare pyramidal geometry (τ₅ = 0.350(6)) (Figure 2).

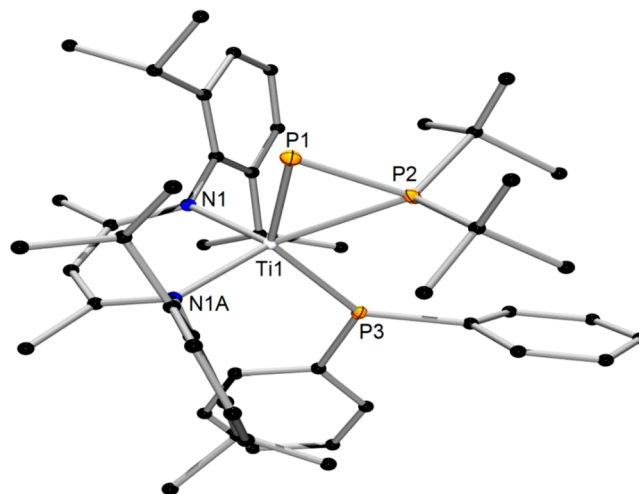


Figure 2. Molecular structure of [Me₂NacNacTi(PPh₂)](η²-P-PtBu₂) (**1**); hydrogen atoms have been omitted for clarity. Important bond lengths (Å) and bond angles (deg): Ti1–N1 2.088(2), Ti1–P1 2.308(5), Ti1–P2 2.573(6), Ti1–P3 2.384(9), P1–P2 2.091(8); P1–P2–Ti1 58.22(3), N1–Ti1–N1A 93.42(10), P2–P1–Ti1 71.40(4), P1–Ti1–P3 135.15(4), P2–Ti1–P3 84.80(3); τ₅(Ti) = 0.350(6) (calculated according to the literature method).⁶²

The obtained molecular structure confirms the nucleophilic attack of the Ph₂P ion on the titanium center, resulting in the elimination of the chloride ion as LiCl. The Ti1–P1 and Ti1–P2 distances (2.308(5) and 2.573(5) Å) are typical for Ti–PP distances in side-on coordination and are comparable to the distances observed in [Me₂NacNacTi(Cl)](η²-P-PtBu₂) (2.3160(7) and 2.5590(7) Å)³⁷ and [Me₂NacNacTi(Cl)](η²-P(Ph)*t*Bu)] (2.3237(7) and 2.5128(7) Å).⁶³ The Ti1–P3 bond (2.384(9) Å) lies in the range between single and double Ti–P bonds and is comparable to the distance (Ti–P*i*Pr₂) observed in [(PNP)Ti]₂(P*i*Pr₂)(μ²-H)₃] (2.385(3) Å) and dramatically shorter than the Ti–P distances observed in complexes: Cp₂TiPPh₂(PMe₃) (2.681(3) Å) and [Li(TMEDA)₂][Cp₂Ti(PPh₂)₂] (2.709(1) and 2.676(1) Å).⁶⁴ The planar coordination of the P3 phosphorus atom (ΣP3 =

360.0(14)°) and the DFT Mayer bond order (MBO) calculations for **1** confirm the double-bond character of the interaction between Ti1 and P3 (1.261 Å) (see Figure S46). Similarly, the planar coordination of the phosphido ligand PPh₂ to the metal center was observed in tungsten and thallium complexes ([Cp*WH(PPh₂)₂(PMe₃)]⁶⁵ and [Cp*Ta(μ-PPh₂)₂(PPh₂)₂]⁶⁶). The NCCCN unsaturated backbone of the β-diketimate ligand is almost planar, with a deviation of 0.072(2) Å from planarity. The titanium atom is out of the plane of the diamine ligand framework by 0.236(7) Å.

Crystals of **2** suitable for X-ray diffraction were grown from a diethyl ether solution and crystallized in the monoclinic space group *P*₂₁/*n*. An X-ray diffraction study established that **2** adopts an ionic structure. The titanium atom is five-coordinate and adopts a pseudosquare pyramidal geometry. The P1, P2, N1, and N2 atoms lie in the plane (rms deviation from the planarity for the P1, P2, N1, and N2 atoms is 0.3107 Å), while the chloride ion occupies an axial position (Figure 3).

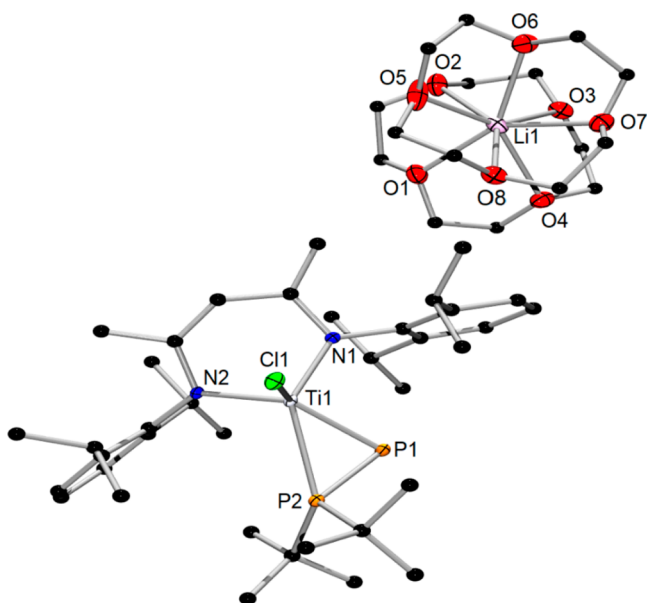


Figure 3. Molecular structure of [MeNacNacTi(Cl){η²-P-PtBu₂}]⁻ [Li(12-crown-4)]⁺ (**2**); hydrogen atoms have been omitted for clarity. Important bond lengths (Å) and bond angles (deg): Ti1–Cl1 2.3329(18), Ti1–N1 1.972(4), Ti1–N2 2.002(4), Ti1–P1 2.3353(17), Ti1–P2 2.6075(16), P1–P2 2.1034(19); P1–P2–Ti1 58.26(5), N1–Ti1–N2 98.04(16), P2–P1–Ti1 71.74(6), Cl1–Ti1–P2 96.56(6), Cl1–Ti1–P1 122.22(6); τ₅(Ti) = 0.224 (calculated according to the literature method).⁶²

The crystallographic structure shows that the phosphanylphosphinidene ligand coordinates side-on to the metal center. The Ti1–P1 distance (2.3353(17) Å) lies in the range between single and double Ti–P bonds. The reported distances of single Ti–P bonds are 2.585(1) Å for [Cp₂Ti(CO)(PEt)₃]⁶⁷ and 2.6060(7) Å for [Ti(2,4-C₇H₁₁)₂(PEt₃)],⁴⁴ while double Ti=P bond distances are 2.1644(7) Å in [^tBuNacNacTi=P(Trip)(Me)]¹⁴ and 2.1831(4) Å in [MeNacNacTi=PMe*(CH₂tBu)].⁶¹ The Ti–P distances are comparable to those observed for the β-diketimate titanium(IV) complexes with phosphanylphosphinidene ligands ([MeNacNacTi(Cl){η²-P-PtBu₂}] (2.3160(7) Å) and [MeNacNacTi(Cl){η²-P-PiPr₂}] (2.3182(7) Å)).³⁷ The Ti1–P2 bond distance is typical for a

single bond between phosphorus and titanium atoms. The P–P distance (2.1034(19) Å) lies in the range of double bonds, especially for the side-on coordination of a phosphanylphosphinidene ligand to a metal center. A similar distance was reported for the previously described β-diketimate titanium(IV) complexes with phosphanylphosphinidene ligands.³⁷

Compound **4a** crystallized as red crystals from a toluene/pentane solution. The molecule crystallized in the *P*₂₁/*c* space group with four molecules in the unit cell. **4a** displays a four-coordinate titanium complex with the metal center in a tetrahedral environment (Figure 4).

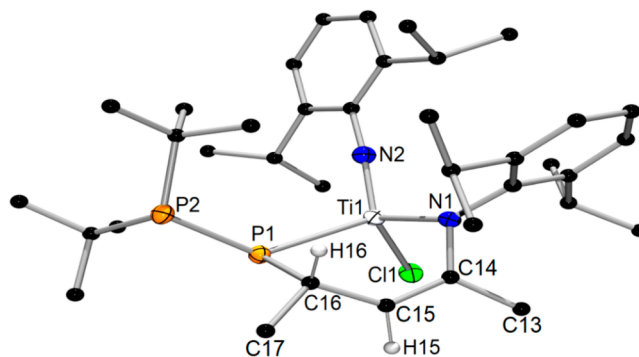


Figure 4. Molecular structure of anion [(Ar)NC(Me)=CHC(H)(Me)(P-PtBu₂)}Ti=NAr(Cl)]⁻ of **4a**; hydrogen atoms have been omitted for clarity (besides H15 and H16). Important bond lengths (Å) and bond angles (deg): Ti1–Cl1 2.3340(10), Ti1–N1 1.965(3), Ti1–N2 1.724(3), Ti1–P1 2.4940(9), P1–P2 2.1938(12), N1–C14 1.416(4), C14–C15 1.370(4), C15–C16 1.519(4), C16–P1 1.893(3), C16–H16 1.000(2), N1–Ti1–N2 111.79(12), N1–Ti1–Cl1 107.12(8), N1–Ti1–P1 106.95(8), N2–Ti1–Cl1 109.13(9), N2–Ti1–P1 112.83(9), Ti1–P1–P2 131.69(4); ΣP1 = 322.78(3), ΣP2 = 321.10(15), ΣC16 = 331.40(2); τ₄(Ti) = 0.979 (calculated according to literature method)⁶⁸ and τ₄(Ti) = 0.968 (calculated according to literature method).⁶⁹

The X-ray structure of **4a** clearly displays the migration of the phosphanylphosphinidene moiety to the β-carbon of the MeNacNac⁻ ligand, and the generation of the imide ligand N–Ar. The Ti–N_{imide} distance is very short (1.724(3) Å), indicating multiple bond character. A similar migration was observed by Mindiola and co-workers in [(Ar)NC(Me)CHC(Me)P(Trip)Ti=NAr(CH₂tBu)], [(Ar)NC(Me)CHC(Me)P(Trip)(CH₂tBu)Ti=NAr(OEt₂)], and [(Ar)NC(Me)CHC(Me)P(Cy)-(CH₂tBu)Ti=NAr(OEt₂)].⁶¹ In **4a**, the NCCCP backbone is not planar, and the reduced carbon atom C16 shows a tetrahedral coordination environment (ΣC16 = 331.40(2)°). The H16 atom was localized according to the electron density map (C–H distance is 1.000(2) Å). The N1–C14 distance of 1.416(4) Å is shorter than typical N–C single bonds (1.48 Å) but is comparable to that observed in the reduced ligand reported by Uhl (N–C 1.428(3) Å and 1.425(3) Å)⁶⁰ and is significantly longer than the N–C distances in delocalized π-bonding systems of nonreduced β-diketimate ligands [(NacNac)Ti(OAr)]₂(μ²:η²:η²-P₂), 1.330, 1.348, 1.367, and 1.341 Å.¹⁷ The C14–C15 bond length of 1.370(4) Å is slightly longer than the distances presented in the literature [(^tBuMesNacNacH)Ge]: 1.344(2) Å⁷⁰ and (Ph₂nacnac)Al[N(Ph)-C(H)(Me)-CH=C(Me)-N(Ph)] 1.332(3) Å⁶⁰ but is still in the range of C=C double bonds, which indicates the presence of a localized C–C double bond in the NCCCP skeleton. The Ti1–P1 (2.4940(9) Å) and P1–P2

(2.1938(12) Å) bond lengths are typical for Ti–P and P–P single bonds.

Crystals of **4b** suitable for X-ray analysis were grown from an diethyl ether/pentane mixture. **4b** crystallizes in the triclinic system in the $P\bar{1}$ space group with two molecules in the unit cell. The molecular structure of **4b** also displays a four-coordinate titanium complex bound to two nitrogen atoms, one chloride, and one phosphorus atom (Figure 5).

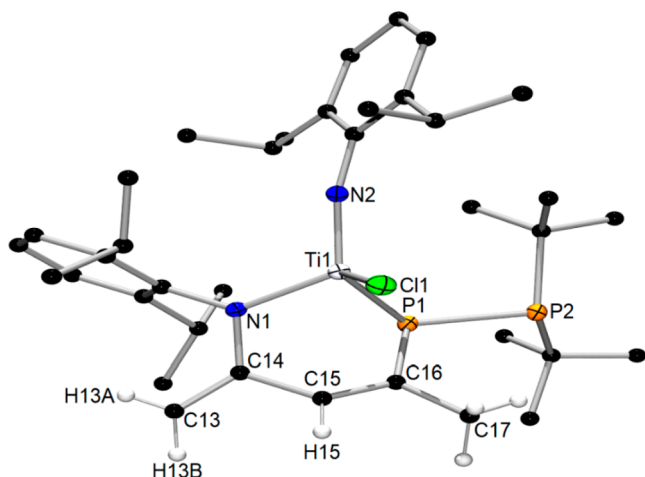


Figure 5. Molecular structure of anion $[\{(\text{Ar})\text{NC}(\text{CH}_2)\text{CH}=\text{C}(\text{Me})(\text{P}-\text{PtBu}_2)\}\text{Ti}=\text{NAr}(\text{Cl})]^-$ of **4b**; hydrogen atoms (besides H13A, H13b, H15, and the methyl protons of the C17 carbon) have been omitted for clarity. Important bond lengths (Å) and bond angles (deg): Ti1–Cl1 2.3387(11), Ti1–N1 1.960(3), Ti1–N2 1.739(3), Ti1–P1 2.4854(11), P1–P2 2.2165(12), N1–C14 1.394(4), C14–C15 1.480(5), C15–C16 1.367(5), C16–P1 1.835(4), C13–C14 1.364(5), C13–H13A 0.98(5), C13–H13B 0.86(5); N1–Ti1–N2 110.87(12), N1–Ti1–Cl1 116.10(9), N1–Ti1–P1 90.46(9), N2–Ti1–Cl1 107.42(10), N2–Ti1–P1 109.59(10), Ti1–P1–P2 117.84(5); $\Sigma\text{P1} = 296.74(3)$, $\Sigma\text{P2} = 310.00(2)$; $\tau_4(\text{Ti}) = 0.904$ (calculated according to literature method)⁶⁸ and $\tau_4'(\text{Ti}) = 0.872$ (calculated according to literature method).⁶⁹

4b confirms the migration of the phosphanylphosphinidene group to the β -carbon of the $\text{Me}^{\text{Me}}\text{NacNac}^-$ ligand and the formation of the imide ligand N–Ar (Ti–N_{imide}, Ti1–N2 1.739(3) Å). In **4b**, the C14, C15, C16, P1, and P2 atoms lie in the plane with rms deviations from planarity of 0.0105 Å. The P2 and N1 atoms deviate very slightly from the plane of C14, C15, C16, and P1 (0.348(2) and 0.788(4) Å, respectively), while the titanium atom deviates very slightly from the plane (by 1.962(3) Å). The C13–C14 (1.364(5) Å) and C15–C16 (1.367(5) Å) distances are comparable to the distances observed in the deprotonated β -diketiminato ligand ($[\{(\text{N}(\text{Ph})-\text{C}(\text{CH}_2)-\text{CH}=\text{C}(\text{Me})-\text{N}(\text{Ph})\}\text{Nb}(\text{N}t\text{Bu})(\text{Ph})] 1.352(7)$ and $1.373(7)$ Å³² and in $[\{(\text{N}(2,6\text{-}i\text{Pr}_2\text{Ph})-\text{C}(\text{CH}_2)-\text{CH}=\text{C}(\text{Me})-\text{N}(2,6\text{-}i\text{Pr}_2\text{Ph})\}\text{Ge}\{\text{N}(\text{SiMe}_3)_2\}] 1.354(3)$ and $1.361(3)$ Å, respectively).⁷¹ The short C–C distances in the organic ligand confirm the presence of localized C=C double bonds; furthermore, the electron density near the C13 atom suggests that the carbon atom is sp^2 -hybridized. In view of this, both H atoms connected to C13 were localized based on the electron density map. Moreover, the distances between the Ti atom and the olefinic carbons (Ti1–C14 2.755(4) Å, Ti1–C15 2.768(3) Å, and Ti1–C16 2.655(4) Å) suggest that there are no close Ti–C interactions in **4b**. Close interactions were observed in $[(\text{Ar})\text{NC}(\text{Me})\text{CHC}(\text{Me})\text{P}(\text{Trip})(\text{CH}_2t\text{Bu})\text{Ti}=\text{NAr}(\text{OEt}_2)]$, as the related distances were 2.420(8) and 2.456(9) Å.⁶¹ The P1–P2 distance (2.2165(12) Å) is typical for a P–P single bond and is slightly longer than those observed in previously described terminal phosphanylphosphido complexes of titanium ($[(\text{PNP})\text{Ti}(\text{Cl})\{\eta^1\text{-P}(\text{SiMe}_3)\text{-PtBu}_2\}]$ (2.1961(9) Å),³⁸ zirconium ($[\text{Ind}_2\text{Zr}(\text{Cl})\{\eta^1\text{-P}(\text{SiMe}_3)\text{-PtBu}_2\}]$ (2.201(1) Å),⁴¹ and $[\text{Cp}_2\text{Zr}(\text{Cl})\{\eta^1\text{-P}(\text{SiMe}_3)\text{-PtBu}_2\}]$ (2.187(2) Å)) and hafnium ($[\text{Cp}_2\text{Hf}(\text{Cl})\{\eta^1\text{-P}(\text{SiMe}_3)\text{-PtBu}_2\}]$ (2.185(1) Å)).⁴⁰ The geometry around P1 and P2 atoms is clearly pyramidal ($\Sigma\text{P1} = 296.72^\circ$ and $\Sigma\text{P2} = 310.04^\circ$).

The X-ray structure of **4a** clearly indicates two stereocenters in the molecule, the δ -carbon and titanium atom, while in complex **4b**, only the titanium atom is stereocenter. The $^31\text{P}\{\text{H}\}$ NMR spectra of **4a** reveal the presence of only one set of resonances. This means that this solution contains a racemic mixture of two diastereomers or that the configuration at the Ti-center is not rigid in solution.

The X-ray structure of **4a** clearly indicates two stereocenters in the molecule, the δ -carbon and titanium atom, while in complex **4b**, only the titanium atom is stereocenter. The $^31\text{P}\{\text{H}\}$ NMR spectra of **4a** reveal the presence of only one set of resonances. This means that this solution contains a racemic mixture of two diastereomers or that the configuration at the Ti-center is not rigid in solution.

4. CONCLUSIONS

We demonstrated two important reaction pathways of $[\text{Me}^{\text{Me}}\text{NacNacTi}(\text{Cl})\{\eta^2\text{-P}(\text{SiMe}_3)\text{-PtBu}_2\}]$ with nucleophiles (Ph_2PLi , $t\text{BuOLi}$, $(\text{Me}_3\text{Si})_2\text{NLi}$, and $t\text{BuNLi}$) in the presence of 12-crown-4, and the reaction outcome depends on the solvent. In toluene, substitution and simultaneous oxidation of titanium occurs with all nucleophiles. Ph_2PLi afforded the most substitution product, and $[\text{Me}^{\text{Me}}\text{NacNacTi}(\text{PPh}_2)\{\eta^2\text{-P-PtBu}_2\}]$ (**1**) was isolated. $[\text{Me}^{\text{Me}}\text{NacNacTi}(\text{Cl})\{\eta^2\text{-P-PtBu}_2\}]^-[\text{Li}(12\text{-crown-4})_2]^+$ (**2**) was isolated for all nucleophiles. Additionally, using fairly harsh crystallization, we also received a $2e^-$ reduction product, $[\{\text{ArNC}(\text{Me})\text{CHC}(\text{Me})\}\text{Ti}=\text{NAr}\{\eta^1\text{-P}(\text{SiMe}_3)\text{-PtBu}_2\}]^-[\text{Li}(12\text{-crown-4})_2]^+$ (**3**), which completes the stoichiometry of the reaction and allows us to understand occurring processes in a nonpolar solvent. However, the same protocol with the same molar ratio but in THF solution led to two different Ti(IV) products, **4a** and **4b**. In both complexes (**4a** and **4b**), the “phospha-Staudinger” displacement in the β -diketiminato ligand and formation of a four-coordinate titanium complexes with the NP ligands was observed. Furthermore, X-ray and NMR spectroscopic investigations revealed that the titanium atoms in both complexes are oxidized and that the organic $\text{Me}^{\text{Me}}\text{NacNac}$ ligands are reduced. The two redox processes are connected with a transfer of one hydrogen atom: In **4b**, the Me group attached to the β -carbon is dehydrogenated, while in **4a**, a hydrogen adds to the δ -carbon of the NP hybrid ligand. We also demonstrated that ionic complex **2** is unstable in THF solution and is transformed to complexes **4a** and **4b**.

■ ASSOCIATED CONTENT

Supporting Information

The Supporting Information is available free of charge at <https://pubs.acs.org/doi/10.1021/acs.inorgchem.0c00824>.

NMR spectroscopic data, crystallographic data, and DFT calculations (PDF)

Accession Codes

CCDC 1859187, 1859190, 1859191, 1991067, and 2001101 contain the supplementary crystallographic data for this paper. These data can be obtained free of charge via www.ccdc.cam.ac.uk/data_request/cif, or by emailing data_request@ccdc.cam.ac.uk, or by contacting The Cambridge Crystallographic

Data Centre, 12 Union Road, Cambridge CB2 1EZ, UK; fax: +44 1223 336033.

AUTHOR INFORMATION

Corresponding Author

L. Ponikiewski – Department of Inorganic Chemistry, Chemical Faculty, Gdansk University of Technology, 80-233 Gdansk, Poland; orcid.org/0000-0002-5037-1956; Email: lukasz.ponikiewski@pg.edu.pl

Authors

A. Ziolkowska – Department of Inorganic Chemistry, Chemical Faculty, Gdansk University of Technology, 80-233 Gdansk, Poland; orcid.org/0000-0001-9818-719X

N. Szykiewicz – Department of Inorganic Chemistry, Chemical Faculty, Gdansk University of Technology, 80-233 Gdansk, Poland; orcid.org/0000-0002-2390-2512

J. Pikies – Department of Inorganic Chemistry, Chemical Faculty, Gdansk University of Technology, 80-233 Gdansk, Poland

Complete contact information is available at: <https://pubs.acs.org/10.1021/acs.inorgchem.0c00824>

Notes

The authors declare no competing financial interest.

ACKNOWLEDGMENTS

Ł.P. thanks the Dean of Chemical Faculty for financial support (DS 033154). Ł.P. and A.Z. thank K. Kaniewska for the help with synthesis of Ph₂PLi. The authors thank PL-Grid Infrastructure and the TASK Computational Center for access to the computational resources.

REFERENCES

- (1) Aktaş, H.; Slootweg, J. C.; Lammertsma, K. Nucleophilic Phosphinidene Complexes: Access and Applicability. *Angew. Chem., Int. Ed.* **2010**, *49* (12), 2102–2113.
- (2) Bailey, B. C.; Huffman, J. C.; Mendiola, D. J.; Weng, W.; Ozerov, O. V. Remarkably Stable Titanium Complexes Containing Terminal Alkylidene, Phosphinidene, and Imide Functionalities. *Organometallics* **2005**, *24* (7), 1390–1393.
- (3) Beckhaus, R. Carbenoid Complexes of Electron Deficient Transition Metals—Syntheses of and with Short Lived Building Blocks. *Angew. Chem., Int. Ed. Engl.* **1997**, *36* (7), 686–713.
- (4) Carroll, M. E.; Pinter, B.; Carroll, P. J.; Mendiola, D. J. Mononuclear and Terminally Bound Titanium Nitrides. *J. Am. Chem. Soc.* **2015**, *137* (28), 8884–8887.
- (5) Davis-Gilbert, Z. W.; Wen, X.; Goodpaster, J. D.; Tonks, I. A. Mechanism of Ti-Catalyzed Oxidative Nitrene Transfer in [2 + 2 + 1] Pyrrole Synthesis from Alkynes and Azobenzene. *J. Am. Chem. Soc.* **2018**, *140* (23), 7267–7281.
- (6) Grant, L. N.; Pinter, B.; Kurogi, T.; Carroll, M. E.; Wu, G.; Manor, B. C.; Carroll, P. J.; Mendiola, D. J. Molecular titanium nitrides: nucleophiles unleashed. *Chem. Sci.* **2017**, *8* (2), 1209–1224.
- (7) Hazari, N.; Mountford, P. Reactions and Applications of Titanium Imido Complexes. *Acc. Chem. Res.* **2005**, *38* (11), 839–849.
- (8) Heins, S. P.; Wolczanski, P. T.; Cundari, T. R.; MacMillan, S. N. Redox non-innocence permits catalytic nitrene carbonylation by (dadi)Ti = NAd (Ad = adamantyl). *Chem. Sci.* **2017**, *8* (5), 3410–3418.
- (9) Kafizas, A.; Carmalt, C. J.; Parkin, I. P. CVD and precursor chemistry of transition metal nitrides. *Coord. Chem. Rev.* **2013**, *257* (13), 2073–2119.
- (10) Kurogi, T.; Won, J.; Park, B.; Trofymchuk, O. S.; Carroll, P. J.; Baik, M.-H.; Mendiola, D. J. Room temperature olefination of

methane with titanium–carbon multiple bonds. *Chem. Sci.* **2018**, *9* (13), 3376–3385.

(11) Osseili, H.; Truong, K.-N.; Spaniol, T. P.; Maron, L.; Englert, U.; Okuda, J. Titanium Carbene Complexes Stabilized by Alkali Metal Amides. *Angew. Chem., Int. Ed.* **2019**, *58* (6), 1833–1837.

(12) Pearce, A. J.; See, X. Y.; Tonks, I. A. Oxidative nitrene transfer from azides to alkynes via Ti(II)/Ti(IV) redox catalysis: formal [2 + 2+1] synthesis of pyrroles. *Chem. Commun.* **2018**, *54* (50), 6891–6894.

(13) Takeda, T. Titanium carbene complexes as useful tools in organic synthesis. *Chem. Rec.* **2007**, *7* (1), 24–36.

(14) Zhao, G.; Basuli, F.; Kilgore, U. J.; Fan, H.; Aneetha, H.; Huffman, J. C.; Wu, G.; Mendiola, D. J. Neutral and Zwitterionic Low-Coordinate Titanium Complexes Bearing the Terminal Phosphinidene Functionality. Structural, Spectroscopic, Theoretical, and Catalytic Studies Addressing the Ti–P Multiple Bond. *J. Am. Chem. Soc.* **2006**, *128* (41), 13575–13585.

(15) Beckhaus, R.; Santamaria, C. Carbene complexes of titanium group metals—formation and reactivity. *J. Organomet. Chem.* **2001**, *617–618*, 81–97.

(16) Basuli, F.; Bailey, B. C.; Tomaszewski, J.; Huffman, J. C.; Mendiola, D. J. A Terminal and Four-Coordinate Titanium Alkylidene Prepared by Oxidatively Induced α -Hydrogen Abstraction. *J. Am. Chem. Soc.* **2003**, *125* (20), 6052–6053.

(17) Grant, L. N.; Pinter, B.; Manor, B. C.; Suter, R.; Grützmacher, H.; Mendiola, D. J. A Planar Ti₂P₂ Core Assembled by Reductive Decarbonylation of α -O–C \equiv P and P–P Radical Coupling. *Chem. - Eur. J.* **2017**, *23* (26), 6272–6276.

(18) Grubba, R.; Kaniewska, K.; Ponikiewski, Ł.; Cristóvão, B.; Ferenc, W.; Dragulescu-Andrasi, A.; Krzyszek, J.; Stoian, S. A.; Pikies, J. Synthetic, Structural, and Spectroscopic Characterization of a Novel Family of High-Spin Iron(II) [(β -Diketiminato)-(phosphanylphosphido)] Complexes. *Inorg. Chem.* **2017**, *56* (18), 11030–11042.

(19) Sakhaei, Z.; Kundu, S.; Donnelly, J. M.; Bertke, J. A.; Kim, W. Y.; Warren, T. H. Nitric oxide release via oxygen atom transfer from nitrite at copper(ii). *Chem. Commun.* **2017**, *53* (3), 549–552.

(20) Webb, D. J.; Fitchett, C. M.; Lein, M.; Fulton, J. R. Carbodiimides as catalysts for the reduction of a cadmium hydride complex. *Chem. Commun.* **2018**, *54* (5), 460–462.

(21) Bourget-Merle, L.; Lappert, M. F.; Severn, J. R. The Chemistry of β -Diketiminato-metal Complexes. *Chem. Rev.* **2002**, *102* (9), 3031–3066.

(22) Webster, R. L. β -Diketiminato complexes of the first row transition metals: applications in catalysis. *Dalton Trans.* **2017**, *46* (14), 4483–4498.

(23) Camp, C.; Arnold, J. On the non-innocence of “Nacnac”: ligand-based reactivity in β -diketiminato supported coordination compounds. *Dalton Trans.* **2016**, *45* (37), 14462–14498.

(24) Phillips, A. D. X β -Diketiminato complexes of groups 3 to 5. *Organomet. Chem.* **2014**, *39*, 72–147.

(25) Basuli, F.; Huffman, J. C.; Mendiola, D. J. Reactivity at the β -Diketiminato Ligand Nacnac- on Titanium(IV) (Nacnac- = [Ar]NC-(CH₃)CHC(CH₃)N[Ar], Ar = 2,6-[CH(CH₃)₂]₂C₆H₃). Diimine-alkoxo and Bis-anilido Ligands Stemming from the Nacnac- Skeleton. *Inorg. Chem.* **2003**, *42* (24), 8003–8010.

(26) Hitchcock, P. B.; Lappert, M. F.; Nycz, J. E. Synthesis, structure and reductive dechlorination of the C-centred phosphorus(iii) [small beta]-diketiminato PCl(Ph)L [L = C{C(Me)NC₆H₃Pri₂-2,6}{C(Me)NHC₆H₃Pri₂-2,6}]. *Chem. Commun.* **2003**, No. 10, 1142–1143.

(27) Abdalla, J. A. B.; Riddlestone, I. M.; Tirfoin, R.; Aldridge, S. Cooperative Bond Activation and Catalytic Reduction of Carbon Dioxide at a Group 13 Metal Center. *Angew. Chem., Int. Ed.* **2015**, *54* (17), 5098–5102.

(28) Basuli, F.; Bailey, B. C.; Huffman, J. C.; Mendiola, D. J. Intramolecular C–H Activation Reactions Derived from a Terminal Titanium Neopentylidene Functionality. Redox-Controlled 1,2-Addition and α -Hydrogen Abstraction Reactions. *Organometallics* **2005**, *24* (13), 3321–3334.

(29) Chu, T.; Vyboishchikov, S. F.; Gabidullin, B. M.; Nikonov, G. I. Unusual Reactions of NacNacAl with Urea and Phosphine Oxides. *Inorg. Chem.* **2017**, *56* (10), 5993–5997.

(30) Hitchcock, P. B.; Lappert, M. F.; Protchenko, A. V. New reactions of β -diketiminatolanthanoid complexes: sterically induced self-deprotonation of β -diketiminato ligands. *Chem. Commun.* **2005**, No. 7, 951–953.

(31) Adhikari, D.; Basuli, F.; Orlando, J. H.; Gao, X.; Huffman, J. C.; Pink, M.; Mindiola, D. J. Zwitterionic and Cationic Titanium and Vanadium Complexes Having Terminal M–C Multiple Bonds. The Role of the β -Diketiminato Ligand in Formation of Charge-Separated Species. *Organometallics* **2009**, *28* (14), 4115–4125.

(32) Camp, C.; Grant, L. N.; Bergman, R. G.; Arnold, J. Photoactivation of d0 niobium imido azides: en route to nitrido complexes. *Chem. Commun.* **2016**, *52* (32), 5538–5541.

(33) Bai, G.; Wei, P.; Stephan, D. W. Reductions of β -Diketiminato–Titanium(III) Complexes. *Organometallics* **2006**, *25* (10), 2649–2655.

(34) Basuli, F.; Bailey, B. C.; Watson, L. A.; Tomaszewski, J.; Huffman, J. C.; Mindiola, D. J. Four-Coordinate Titanium Alkylidene Complexes: Synthesis, Reactivity, and Kinetic Studies Involving the Terminal Neopentylidene Functionality. *Organometallics* **2005**, *24* (8), 1886–1906.

(35) Basuli, F.; Huffman, J. C.; Mindiola, D. J. Reductive C–N bond cleavage of the NCCCN β -diketiminato backbone: A direct approach to azabutadienyl and alkylidene-anilide scaffolds. *Inorg. Chim. Acta* **2007**, *360* (1), 246–254.

(36) Hamaki, H.; Takeda, N.; Tokitoh, N. Nucleophilic Attack toward Group 4 Metal Complexes Bearing Reactive 1-Aza-1,3-butadienyl and Imido Moieties. *Inorg. Chem.* **2007**, *46* (5), 1795–1802.

(37) Ponikiewski, Ł.; Ziółkowska, A.; Pikies, J. Reactions of lithiated diphosphanes $\text{R}_2\text{P-P}(\text{SiMe}_3)\text{Li}$ ($\text{R} = t\text{Bu}$ and $i\text{Pr}$) with $[\text{M}^c\text{NacnacTiCl}_2\text{xTHF}]$ and $[\text{M}^c\text{NacnacTiCl}_3]$. Formation and bearing the side-on phosphanylphosphido and phosphanylphosphinidene functionalities. *Inorg. Chem.* **2017**, *56*, 1094–1103.

(38) Ponikiewski, Ł.; Ziółkowska, A.; Zauliczny, M.; Pikies, J. Reactions of lithiated diphosphanes $\text{R}_2\text{P-P}(\text{SiMe}_3)\text{Li-nTHF}$ ($\text{R} = t\text{Bu}$, $i\text{Pr}$) with $[(\text{PNP})\text{TiCl}_2]$. Two different coordination types of phosphanylphosphido ligand to the metal center. *Polyhedron* **2017**, *137*, 182–187.

(39) Ziółkowska, A.; Szykiewicz, N.; Wiśniewska, A.; Pikies, J.; Ponikiewski, Ł. Reactions of $(\text{Ph})t\text{BuP-P}(\text{SiMe}_3)\text{Li}\cdot 3\text{THF}$ with $[(\text{PNP})\text{TiCl}_2]$ and $[\text{M}^c\text{NacnacTiCl}_2\cdot\text{THF}]$: synthesis of first PNP titanium(IV) complex with the phosphanylphosphinidene ligand $[(\text{PNP})\text{Ti}(\text{Cl})\{\eta^2\text{-P-P}(\text{Ph})t\text{Bu}\}]$. *Dalton Transactions* **2018**, *47* (29), 9733–9741.

(40) Grubba, R.; Wiśniewska, A.; Baranowska, K.; Matern, E.; Pikies, J. General route for the synthesis of terminal phosphanylphosphido complexes of Zr(IV) and Hf(IV): Structural investigations of the first zirconium complex with a phosphanylphosphido ligand. *Polyhedron* **2011**, *30* (7), 1238–1243.

(41) Łapczuk-Krygier, A.; Baranowska, K.; Ponikiewski, Ł.; Matern, E.; Pikies, J. π -Indenyl substituted zirconium compounds containing terminal bonded phosphanylphosphido ligands $[\text{Ind}_2\text{Zr}(\text{Cl})\{\text{(Me}_3\text{Si)-P-PR}_2\text{-}\kappa\text{P1}\}]$. Synthesis, X-ray analysis and NMR studies. *Inorg. Chim. Acta* **2012**, *387*, 361–365.

(42) Zauliczny, M.; Grubba, R.; Ponikiewski, Ł.; Pikies, J. Phosphanylphosphido and phosphanylphosphinidene complexes of zirconium(IV) supported by bidentate N,N ligands. *Polyhedron* **2017**, *123*, 353–360.

(43) Grubba, R.; Baranowska, K.; Gudat, D.; Pikies, J. Reactions of Lithiated Diphosphanes $\text{R}_2\text{P-P}(\text{SiMe}_3)\text{Li}$ ($\text{R} = t\text{Bu}$, $i\text{Pr}$, $i\text{Pr}_2\text{N}$, Et_2N) with $[\text{Cp}_2\text{WCl}_2]$. Syntheses and Structures of the First Terminal Phosphanylphosphido Complexes of Tungsten(IV). *Organometallics* **2011**, *30* (24), 6655–6660.

(44) Kruczynski, T.; Grubba, R.; Baranowska, K.; Pikies, J. Syntheses and structures of the first terminal phosphanylphosphido complexes of molybdenum(IV). *Polyhedron* **2012**, *39* (1), 25–30.

(45) Pikies, J.; Baum, E.; Matern, E.; Chojnacki, J.; Grubba, R.; Robaszekiewicz, A. A new synthetic entry to phosphinophosphinidene complexes. Synthesis and structural characterisation of the first side-on bonded and the first terminally bonded phosphinophosphinidene zirconium complexes $[\mu\text{-}(1,2\text{-}\eta\text{-}t\text{Bu}_2\text{P} = \text{P})\{\text{Zr}(\text{Cl})\text{Cp}_2\}_2]$ and $[\{\text{Zr}(\text{PPhMe}_2)\text{Cp}_2\}(\eta^1\text{-P-P}t\text{Bu}_2)]$. *Chem. Commun.* **2004**, No. 21, 2478–2479.

(46) Grubba, R.; Baranowska, K.; Chojnacki, J.; Pikies, J. Access to Side-On Bonded Tungsten Phosphanylphosphinidene Complexes. *Eur. J. Inorg. Chem.* **2012**, *2012* (20), 3263–3265.

(47) Grubba, R.; Ordyszewska, A.; Kaniewska, K.; Ponikiewski, Ł.; Chojnacki, J.; Gudat, D.; Pikies, J. Reactivity of Phosphanylphosphinidene Complex of Tungsten(VI) toward Phosphines: A New Method of Synthesis of catena-Polyphosphorus Ligands. *Inorg. Chem.* **2015**, *54* (17), 8380–8387.

(48) Grubba, R.; Wiśniewska, A.; Ponikiewski, Ł.; Caporali, M.; Peruzzini, M.; Pikies, J. Reactivity of Diimido Complexes of Molybdenum and Tungsten towards Lithium Derivatives of Diphosphanes and Triphosphanes. *Eur. J. Inorg. Chem.* **2014**, *2014* (10), 1811–1817.

(49) Domanska-Babul, W.; Chojnacki, J.; Matern, E.; Pikies, J. Reactions of $\text{R}_2\text{P-P}(\text{SiMe}_3)\text{Li}$ with $[(\text{R}_3\text{P})_2\text{PtCl}_2]$. A general and efficient entry to phosphanylphosphinidene complexes of platinum. Syntheses and structures of $[(\eta^2\text{-P} = \text{P}i\text{Pr}_2)\text{Pt}(\text{p-Tol}_3\text{P})_2]$, $[(\eta^2\text{-P} = \text{P}t\text{Bu}_2)\text{Pt}(\text{p-Tol}_3\text{P})_2]$, $[(\eta^2\text{-P} = \text{P}(\text{NiPr}_2)_2)\text{Pt}(\text{p-Tol}_3\text{P})_2]$ and $[(\text{Et}_2\text{PhP})_2\text{Pt}]_2$. *Dalton Trans.* **2009**, No. 1, 146–151.

(50) Konitz, A.; Krautscheid, H.; Pikies, J. (Di-*tert*-butylmethylphosphane)(η^2 -di-*tert*-butylphosphanylphosphinidene)-(triphenylphosphane)platinum(0). *Acta Crystallogr., Sect. C: Cryst. Struct. Commun.* **2009**, *65* (1), m21–m23.

(51) Krautscheid, H.; Matern, E.; Kovacs, I.; Fritz, G.; Pikies, J. Komplexchemie P-reicher Phosphane und Silylphosphane. XIV. Phosphinophosphiniden $t\text{Bu}_2\text{P-P}$ als Ligand in den Pt-Komplexen $[\eta^2\text{-}\{t\text{Bu}_2\text{P-P}\}\text{Pt}(\text{PPh}_3)_2]$ und $[\eta^2\text{-}\{t\text{Bu}_2\text{P-P}\}\text{Pt}(\text{PEtPh}_2)_2]$. *Z. Anorg. Allg. Chem.* **1997**, *623* (12), 1917–1924.

(52) Krautscheid, H.; Matern, E.; Pikies, J.; Fritz, G. Bildung und Struktur des $[\{\eta^2\text{-}t\text{Bu}_2\text{P-P}\}\text{Pt}(\text{PH}t\text{Bu}_2)(\text{PPh}_3)]$. *Z. Anorg. Allg. Chem.* **2000**, *626* (10), 2133–2135.

(53) Grubba, R.; Ordyszewska, A.; Ponikiewski, Ł.; Gudat, D.; Pikies, J. An investigation on the chemistry of the $\text{R}_2\text{P} = \text{P}$ ligand: reactions of a phosphanylphosphinidene complex of tungsten(VI) with electrophilic reagents. *Dalton Trans.* **2016**, *45* (5), 2172–2179.

(54) Hey-Hawkins, E.; Lappert, M. F.; Atwood, J. L.; Bott, S. G. Bis(trimethylsilyl)phosphido complexes. Part 3. Syntheses, structures and reactions of [bis(trimethylsilyl)phosphido]-zirconocene(IV) complexes and the X-ray structure of $\{\text{AlMe}_2[\mu\text{-P}(\text{SiMe}_3)_2]\}_2$. *J. Chem. Soc., Dalton Trans.* **1991**, No. 5, 939–948.

(55) Ziółkowska, A.; Szykiewicz, N.; Pikies, J.; Ponikiewski, Ł. Reactivity study of a β -diketiminato titanium(III) complex with a phosphanylphosphido ligand towards chlorophosphanes. A new method of synthesis of β -diketiminato titanium(IV) complexes with versatile phosphanylphosphinidenes. *Polyhedron* **2019**, *169*, 278–286.

(56) Kaniewska, K.; Dragulescu-Andrasi, A.; Ponikiewski, Ł.; Pikies, J.; Stoian, S. A.; Grubba, R. Syntheses, Structures and Reactivity of Terminal Phosphido Complexes of Iron(II) Supported by a β -Diketiminato Ligand. *Eur. J. Inorg. Chem.* **2018**, *2018* (38), 4298–4308.

(57) Hall, P. L.; Gilchrist, J. H.; Collum, D. B. Effects of lithium salts on the stereochemistry of ketone enolization by lithium 2,2,6,6-tetramethylpiperidide (LiTMP). A convenient method for highly E-selective enolate formation. *J. Am. Chem. Soc.* **1991**, *113* (25), 9571–9574.

(58) Basuli, F.; Kilgore, U. J.; Brown, D.; Huffman, J. C.; Mindiola, D. J. Terminal Zirconium Imides Prepared by Reductive C–N Bond Cleavage. *Organometallics* **2004**, *23* (26), 6166–6175.

(59) Hamaki, H.; Takeda, N.; Tokitoh, N. Reduction of Tetravalent Group 4 Metal Complexes Supported by an Extremely Bulky, Unsymmetrically Substituted β -Diketiminato Ligand Leading to the

Regioselective C = N Bond Cleavage Giving Ring-Contracted Metal-Imido Complexes. *Organometallics* **2006**, *25* (10), 2457–2464.

(60) Jana, B.; Uhl, W. New aluminum and gallium complexes of β -diketiminato and β -ketiminato ligands. *Inorg. Chim. Acta* **2017**, *455*, 61–69.

(61) Basuli, F.; Tomaszewski, J.; Huffman, J. C.; Mindiola, D. J. Four-Coordinate Phosphinidene Complexes of Titanium Prepared by α -H-Migration: Phospha-Staudinger and Phosphaalkene-Insertion Reactions. *J. Am. Chem. Soc.* **2003**, *125* (34), 10170–10171.

(62) Addison, A. W.; Rao, T. N.; Reedijk, J.; van Rijn, J.; Verschoor, G. C. Synthesis, structure, and spectroscopic properties of copper(II) compounds containing nitrogen–sulphur donor ligands; the crystal and molecular structure of aqua[1,7-bis(N-methylbenzimidazol-2'-yl)-2,6-dithiaheptane]copper(II) perchlorate. *J. Chem. Soc., Dalton Trans.* **1984**, No. 7, 1349–1356.

(63) Ziółkowska, A.; Szykiewicz, N.; Wiśniewska, A.; Pikies, J.; Ponikiewski, Ł. Reactions of (Ph)*t*BuP-P(SiMe₃)Li·3THF with [(PNP)TiCl₂] and [Me₂NacNacTiCl₂·THF]: synthesis of first PNP titanium(IV) complex with the phosphanylphosphinidene ligand [(PNP)Ti(Cl){ η^2 -P-P(Ph)*t*Bu}]. *Dalton Trans.* **2018**, *47*, 9733–9741.

(64) Dick, D. G.; Stephan, D. W. Titanocene(III) phosphides: trapping and structure of mononuclear intermediates in the formation of [Cp₂Ti(μ -PR₂)₂]₂. *Organometallics* **1991**, *10* (8), 2811–2816.

(65) Baker, R. T.; Calabrese, J. C.; Harlow, R. L.; Williams, I. D. New (η -C₃Me₃)M(PR₂)_x complexes (M = tantalum, molybdenum, and tungsten): reversible P-H bond activation, sp³ C-H bond activation, and P-C bond formation. *Organometallics* **1993**, *12* (3), 830–841.

(66) Abdul Hadi, G. A.; Fromm, K.; Blaurock, S.; Jelonek, S.; Hey-Hwakins, E. Organometallic tantalum complexes with phosphine, phosphanido and phosphinidene ligands. Syntheses and crystal structures of [Sp'TaCl₄[PH₂(2,4,6-Pr³C₆H₂)]], [Cp'Ta(μ -PPh₂)-(PPh₂)₂·C₇H₈] and [Cp'TaCl[μ -P(2,4,6-Pr³C₆H₂)]]₂·C₇H₈ (Cp' = C₃H₅Me). *Polyhedron* **1997**, *16* (4), 721–731.

(67) Edwards, B. H.; Rogers, R. D.; Sikora, D. J.; Atwood, J. L.; Rausch, M. D. Formation, reactivities, and molecular structures of phosphine derivatives of titanocene. Isolation and characterization of a titanium monoolefin π complex. *J. Am. Chem. Soc.* **1983**, *105* (3), 416–426.

(68) Yang, L.; Powell, D. R.; Houser, R. P. Structural variation in copper(I) complexes with pyridylmethylamide ligands: structural analysis with a new four-coordinate geometry index, τ_4 . *Dalton Trans.* **2007**, No. 9, 955–964.

(69) Okuniewski, A.; Rosiak, D.; Chojnacki, J.; Becker, B. Coordination polymers and molecular structures among complexes of mercury(II) halides with selected 1-benzoylthioureas. *Polyhedron* **2015**, *90*, 47–57.

(70) Choong, S. L.; Woodul, W. D.; Schenk, C.; Stasch, A.; Richards, A. F.; Jones, C. Synthesis, Characterization, and Reactivity of an N-Heterocyclic Germanium(II) Hydride: Reversible Hydrogermylation of a Phosphaalkyne. *Organometallics* **2011**, *30* (20), 5543–5550.

(71) Jana, A.; Roesky, H. W.; Schulzke, C. Reactivity of germanium(II) hydride with nitrous oxide, trimethylsilyl azide, ketones, and alkynes and the reaction of a methyl analogue with trimethylsilyl diazomethane. *Dalton Trans.* **2010**, *39* (1), 132–138.